Natural Resources Canada | Ressources naturelles Canada

GEOLOGICAL SURVEY OF CANADA
OPEN FILE 8356

Mass-failure complexes on the central Beaufort Slope, offshore Northwest Territories

G.D.M. Cameron and E.L. King

2019

Canada

GEOLOGICAL SURVEY OF CANADA
OPEN FILE 8356

Mass-failure complexes on the central Beaufort Slope, offshore Northwest Territories

G.D.M. Cameron and E.L. King

2019

Permanent link: https://doi.org/10.4095/314644

This publication is available for free download through GEOSCAN (http://geoscan.nrcan.gc.ca/).

Recommended citation
Cameron, G.D.M. and King, E.L., 2019. Mass-failure complexes on the central Beaufort Slope, offshore Northwest Territories; Geological Survey of Canada, Open File 8356, 40 p. https://doi.org/10.4095/314644

Publications in this series have not been edited; they are released as submitted by the author.

Table of Contents

ACKNOWLEDGEMENTS

This study was conducted as part of the Natural Resources Canada (NRCan) Public Safety Program, Landslides & Marine Geoscience Project, Beaufort Sea Geohazards Assessment Activity. Multibeam data were collected from CCGS Amundsen in 2009 and 2010 and 3.5kHz sub-bottom profiler data from 2009 to 2014 under the umbrella of the ArcticNet Seabed Mapping Program, with critical support from Patrick Lajunesse, Keith Lesvesque, and Louis Fortier. High resolution multibeam images were collected from CCGS Laurier in 2013 (Humfrey Melling, Fisheries and Oceans Canada and Scott Dallimore, Geological Survey of Canada-Pacific, in Sidney, BC) using an autonomous underwater vehicle and made available through agreements with Charlie Paull, David Caress and co-workers at Monterey Bay Research Aquarium in California. Thanks are also due to the crew of CCGS Amundsen and CCGS Sir Wilfred Laurier. Funding was provided from NRCan through PERD (Program of the Energy Research and Development), the Beaufort Regional Environmental Assessment (BREA) under Aboriginal Affairs and Northern Development Canada (AANDC) and from ExxonMobil Canada Energy and Imperial Oil Resources. The support from many individuals within these institutions was instrumental in collecting, accessing and facilitating interpretations of these data. Thanks are due to Scott Dallimore for reviewing this report.

AUTHORS' ADDRESS

Natural Resources Canada, Geological Survey of Canada (Atlantic), Bedford Institute of Oceanography, P.O. Box 1006, Dartmouth, NS, B2Y 4A2

SUMMARY

Interest in oil and gas exploration and development on the Beaufort Slope raises concerns about the potential slope geohazards. Large mass transport slide complexes have been identified on the Beaufort Slope from multibeam and high-resolution seismic data collected between 2001 and 2010.

Two areas of failed seafloor morphology are identified at mid-slope depths in the Kugmallit Fan Study Area (KF); the Ikit and the Kugmallit slide complexes. These are mid-size failure complexes, consisting of numerous mass transport deposit (MTD) events, encompassing several failure styles. These are the latest of numerous (older and buried) events and are the focus of this study.

The Ikit Slide Valley Complex (SVC), found in the western KF, is about 24 km along the shelf break and about 54 km downslope, with an area of 1897 km^2. Rotational, retrogress and translational failures are the types of mass transport mechanisms identified. Some of these include re-failure within the same complex. Crosscutting relationships show that large portions of the failures in the southern Ikit SVC are older than in the northern Ikit SVC and that at least 5 successsive failure events are distinguished.

The Kugmallit Slide Valley Complex, found in the central KF, is about 68 km long and 14 wide, with an area of 1537 km^2. Following a large evacuation, rotational and retrogressive failures continued with crosscutting relationships showing numerous failure entities across at least 6 events. The Ikit and Kugmallit SVCs may be the upper reaches of one larger event.

Migrating fluids likely preconditioned the sediments in the failure areas though multiple mechanisms are suspected and only broadly known. The widespread occurrence of buried failures indicates a periodic history and suggests that earthquakes were the triggering mechanism in this seismically active area. The occurrence of these failures, in both SVCs, may have been close in time. Absolute age is likely 1000 years or less from several lines of evidence, but further corroborative study is necessary.

INTRODUCTION

Hydrocarbon exploration and drilling activities in the Beaufort Sea began on the continental shelf in 1972 and continued, on and off, until 2006, (Blasco et al., 2012). Starting in 2008 companies became interested in exploring for oil and gas in waters from 100 to 1500 m on the Beaufort slope which has raised concerns about slope geohazards. The mandate for safe operations rests with the National Energy Board and was heightened with prospects of drilling in the late 2010s. Natural Resources Canada has incorporated activities in its Public Safety Geoscience Program to assess and quantify potential geohazards in the region. This report focusses on mass sediment failures occurring in slide valley complexes on the Beaufort Slope, approximately 100km north of Tuktoyaktuk, NWT.

Seabed mapping using multibeam sonar, shallow sub-bottom profiler surveys and seafloor sampling was conducted on the central Beaufort upper slope in 2009, 2010 and 2011, primarily aboard Canadian Coast Guard Ship (CCGS) Amundsen, during ArcticNet expeditions (Figs. 1 and 2). Significant support for these research activities was provided by active hydrocarbon industry licences held in the area. Woodworth-Lynas et al. (2016) identified a variety of potential geohazards including large slope failures in the Kugmallit Fan area. They endeavoured to link geological architecture and process on the slope to what is known on the shelf from earlier studies as an attempt to create a seismo-chronostratigraphic framework.

A locally broad proto-Mackenzie River fed the bathymetrically-defined Kugmallit Fan Study Area (KF), (multibeam area), (Fig. 1). This study area is approximately 8000 km^3 and is located on the upper continental slope between 100 and 1500 m water depth, (Fig. 1). Multibeam coverage in the KF area show surficial expressions of large, mass wasting, slide valley complexes (SVC) that have multiple phases of seabed failures. These SVCs are tens of kilometres wide and more than 60 km long, which join downslope into large regions of accumulated failed sediment, (Fig 3). This report will describe these failures, with an emphasis on their relative timing.

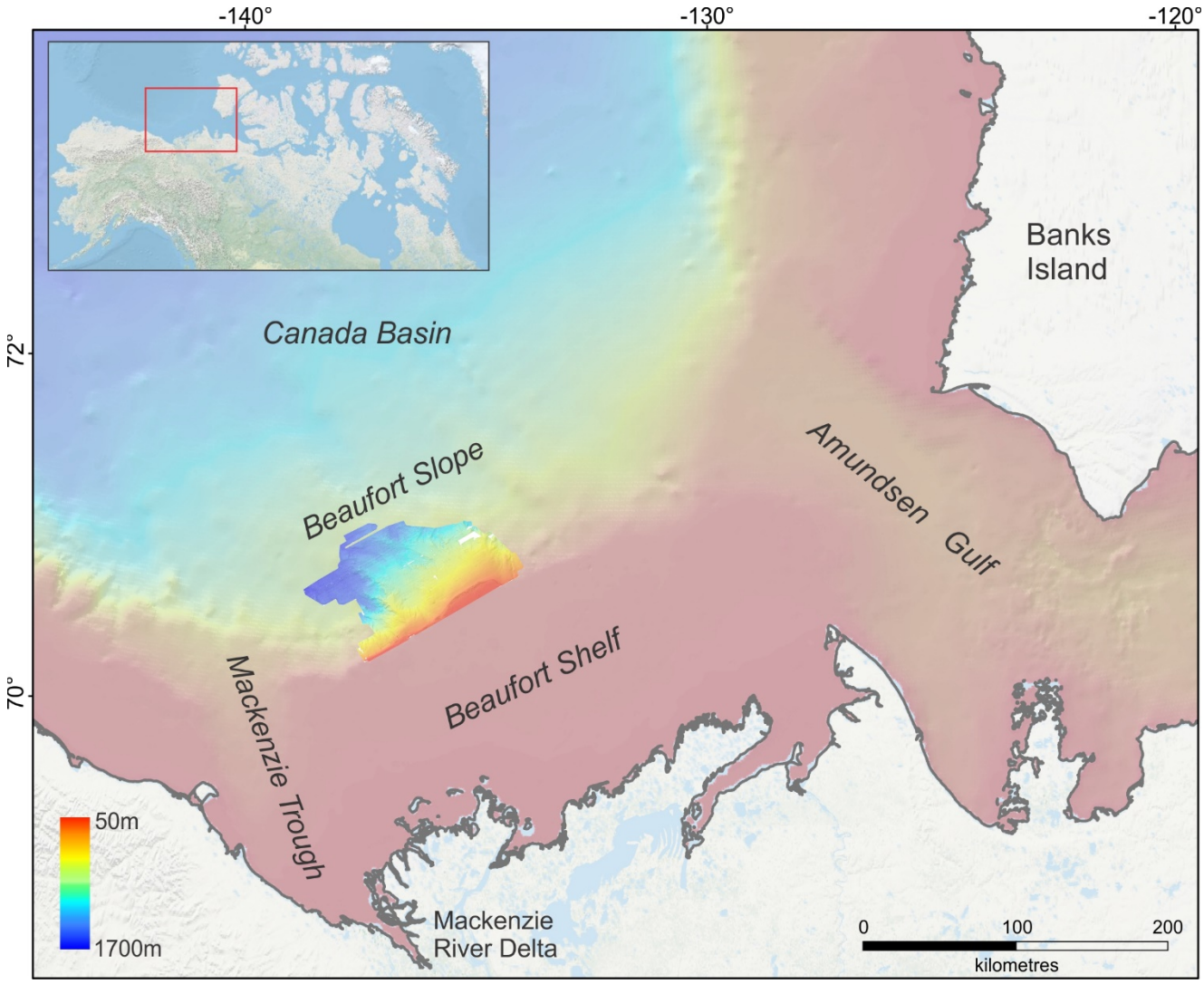

Figure 1. ***The location of the Kugmallit Fan study area is defined by the brightly coloured multibeam mosaic on the Beaufort Slope. Multibeam image was collected by the ArcticNet consortium from CCGS Amundsen in 2009, 2010 and 2011. Colour bar applies only to the multibeam study area.***

GEOGRAPHIC AND GEOLOGICAL SETTING

The Canadian Beaufort Sea reaches from the Alaskan border in the west, to the outermost Amundsen Gulf in the east. The continental shelf is100 km wide, with a shelf break at about 100 m water depth, intersecting a northward dipping continental slope. Identified as the Beaufort Shelf, it is bordered east and west by two large embayments, Amundsen Gulf and Mackenzie Trough, both glacially excavated shelf-crossing troughs which drained a significant portion of the Laurentide Ice Sheet and previous glacial phases (Batchelor et al. 2013, 2014). These and the Mackenzie and proto-Mackenzie River contributed to major sediment supply to the Canada Basin, forming the Mackenzie Fan, as identified by Mosher et al. (2009, 2011). It extends 500 km beyond the shelf break and spans nearly 500 km between Mackenzie Trough and Amundsen Gulf. The Fan is dominated by large and very large mass transport failures and their deposits. A deeply buried one apparently reaching over 15000 km^3 in volume (Mosher et al. 2011), potentially the largest known global occurrence.

The upper continental slope study area has overall gradients of 0.5˚ to 1° with failure scarps exceeding 30^0 (from AUV data)in water depths from 100 to 1500 m. The slope seabed morphology is mostly the result of gravity mass transport processes. These persist downward throughout the Cenozoic section and at most stratigraphic levels in the Quaternary, including at least tens of events in the late and post-glacial sequence (Rohr et al., in prep.). The entire slope seabed morphology is affected by mass transport processes though some are shallowly buried, by up to 10s of metres. The shelf has broad folds and faults at moderate depth (100-1000 m), maintains buried permafrost in varying states of decay, and seabed-situated pingo-like mound and moat features (presently termed pingo-like-features (PLFs)) likely related to this permafrost decay (Dallimore et al. 2015). Other seabed instability structures on the slope are fluid escape features, which have brought sediment to the seafloor. Within the fan is another sedimentary bulge centered on the Beaufort Shelf approximately equidistant between the shelf-crossing troughs, recognized by Rhor (in prep.) as a depocenter dominated by late Cenozoic failures, and known as the Kugmallit Fan. Deep erosion on land with the onset of glaciations marked a change in Mackenzie River flow to it's present northward path (Duk-Rodkin and Hughes 1994) and the Kugmallit Fan may be a precursor (Rohr et al., in prep.) to the present (post-glacial) depocenter, progressively filling the glacially eroded channel cut through the present delta (Blasco et al. 2011) .

The Laurentide Ice Sheet reached its maximum extent on the inner Beaufort Shelf at 18 ka BP (Dyke et al. 2003, Blasco et al. 2011) though evidence for local timing and extent, including its shelf break position, remains unconfirmed in the formal literature. There is some evidence that continental ice sheets crossed the Beaufort shelf, at least filling the shelf-crossing troughs (Rampton 1982, 1988, Murton et al. 2015, Blasco et al. 2011) for short time periods and possibly left the shelf emergent for long periods. The deglacial period resulted in a blanket of glaciomarine sediments which pinch out at the shelf edge, but thicken again (to several 10s of metres) just beyond the shelf break and then thin consistently downslope.

Mackenzie River sediments discharge into the Arctic Ocean and mostly bypass the central shelf, as the Coriolis force drives the sediment east along the inner shelf (Blasco et al. 2012). On the shelf and slope, the top 100 m of sediment is younger than ~27 ka (Hill et al. 1985, Blasco et al. 2011), representing late glacial to Holocene deposition of mostly silts and clays. Sedimentation rates exceeding 600 cm/ka have been estimated for the uppermost Beaufort Slope during post LGM, (Woodworth-Lynas, et al., 2016). Over 700 m of impermeable ice-bearing sediments occur on the Beaufort Shelf and pinch-out at the shelf edge (Blasco et al. 2011). Over 3500 pingos or PLFs (Blasco et al. 2011, King, pers. comm.), some of which clearly involve fluid and gas escape (St. Ange et al. 2014) and some with ice cores (Dallimore and Paull 2015) have been identified at the shelf edge.

Hill, (1985) suggests a maximum lowering of sea level by 70 m at 10 ka BP, with a subsequent rise to the present. Seismicity is usually of a low magnitude with a few historical events greater than magnitude 5 being reported (Lamontagne et al. 2008). However, their proximity to the slide failures are a potential triggering factor.

Present day sediment (mud) to the shelf and slope originates from the Mackenzie River, contributing locally tens of metres thickness just beyond the shelf break in the study area, but a narrow zone of non-deposition and erosion characterizes much of the shelf break (Woodworth-Lynas et al., 2016). This has recently been mapped and attributed to a mid-Holocene evolution of the Beaufort Jet (King et al. 2017), a dominantly west to east contour current which follows the shelf break in the upper 150 m of the water column.

Understanding supply and distribution of recent sediment to the mass failure areas is critical to dating of the failures by recognition of post-failure sedimentation covering the transported material. This is the focus of a parallel study to provide some sense of absolute ages on the failures. Initial results using radiocarbon and Cs/Pb dating techniques confirm the recent failure ages (Cameron et al. 2017) initially suggested (St Ange, 2014) but the details of assigning absolute time to the relative timing established in this study remain elusive.

DATA AND METHODS

Multibeam bathymetry data has been collected in the southern Canadian Beaufort Sea, the bulk between 2001 and 2010, and largely coincident with the hydrocarbon industry license blocks (Fig.2). Agreements among the Geological Survey of Canada (https://www.nrcan.gc.ca/earth-sciences/science/geology/gsc/17100), the Ocean Mapping Group at University of New Brunswick (http://www.omg.unb.ca/), as part of the ArcticNET program (http://www.arcticnet.ulaval.ca/), and largely funded by ExxonMobil Canada, British Petroleum Canada and Imperial Oil Resources Ventures Ltd. facilitated these surveys. Data used for this study were collected using Kongsberg-Simrad 30 kHz EM302 multibeam sonar and Knudsen 3.5 kHz sub-bottom profiler from the research vessels CCGS *Amundsen* and CCGS *Nahidik* (Fig 2 grey line grid). A dense grid of survey-lines was oriented along slope, at 250 or 1000 m intervals, depending on water depth, in order to insure 100% bathymetric coverage.

The EM302 was operated in dual-swath mode and yielded 432 soundings with 288 beams in high density mode. Globally corrected C-Nav dGPS solutions were applied to all data and soundings were reduced to mean sea level using the tidal model WebTide. Vertical resolution varies with water depth and collection systems, but generally was as much as ±5 m at slope water depths of ~1000 m. The datasets were gridded at 10 m horizontal resolution. The multibeam datasets have been combined and compiled both as a single bathymetric coloured shaded relief image, but also viewed in a two-layer mode with the grey-tone shaded relief overlain with a semi-transparent coloured digital elevation model displayed so the full colour range is adjusted dynamically to the map scale.

Knudsen 3.5 kHz sub-bottom profiler data from a USCG Healy 2013 survey were also used in this study. Much of the remainder of the slope, outside the study area, had relatively sparse coverage, in the form of regional survey lines. However, bathymetric coverage, since the 2009-10 surveys, has recently been completed by various institutions, giving continuous upper slope coverage to the US border.

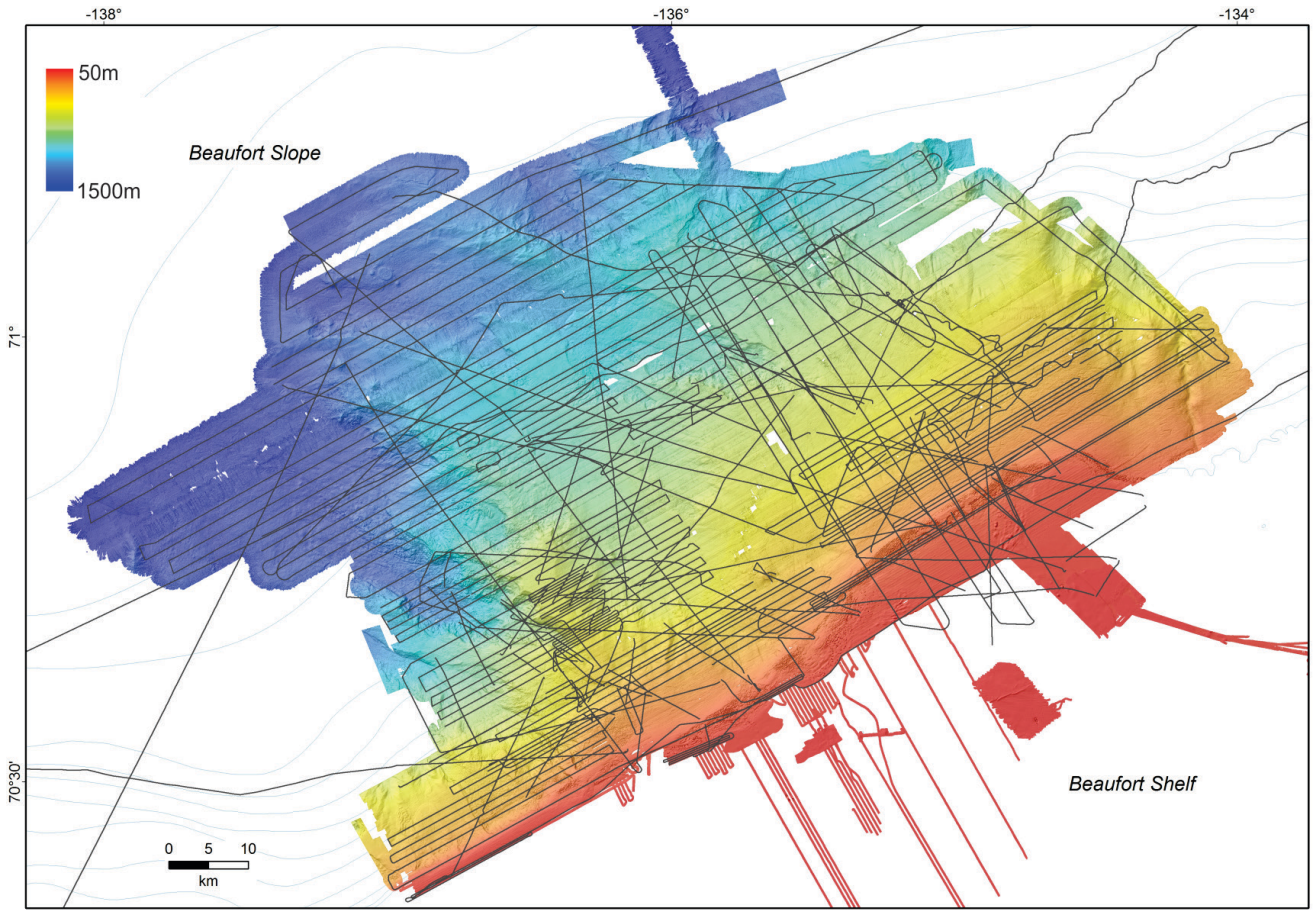

Figure 2. ***Multibeam map of the Kugmallit study area showing the distribution of 3.5 kHz seismic lines (gray lines) used in this study, which were collected during Amundsen cruises 2009804, 2010804, 2011804 and 2014804. Knudsen 3.5 kHz seismic data from Healy2013 were also used. The estimated coverage is greater than 4000 line-kilometres.***

RESULTS

Sediment Instability Features

Figure 3 presents an overview of failed and unfailed sediment and seabed instability features in the study area. These include a large, nearly contiguous SVC and rare smaller and isolated outcropping mass failures (purple), circular mud volcanoes (dark green) and often smooth shelf morphology (light green) which includes areas of complex shelf edge seabed rugosity arising from mounds and ridges of pingo-like features (PLF).

Slide Valley Complexes

The combination of multibeam bathymetry and high-resolution seismic has shown that there are geologically recent, large, complex failures on the Beaufort Slope in the Kugmallit Fan study area (KF) (Fig. 1). The seafloor in the KF has been subdivided into areas of failed (purple) and unfailed sediment (red), (Fig. 3) based primarily on the surficial expression from the multibeam images and an

ability to recognize (or not) a blanket of stratified mud on the 3.5 kHz high-resolution seismic profile data which covers the structurally disturbed slide material.

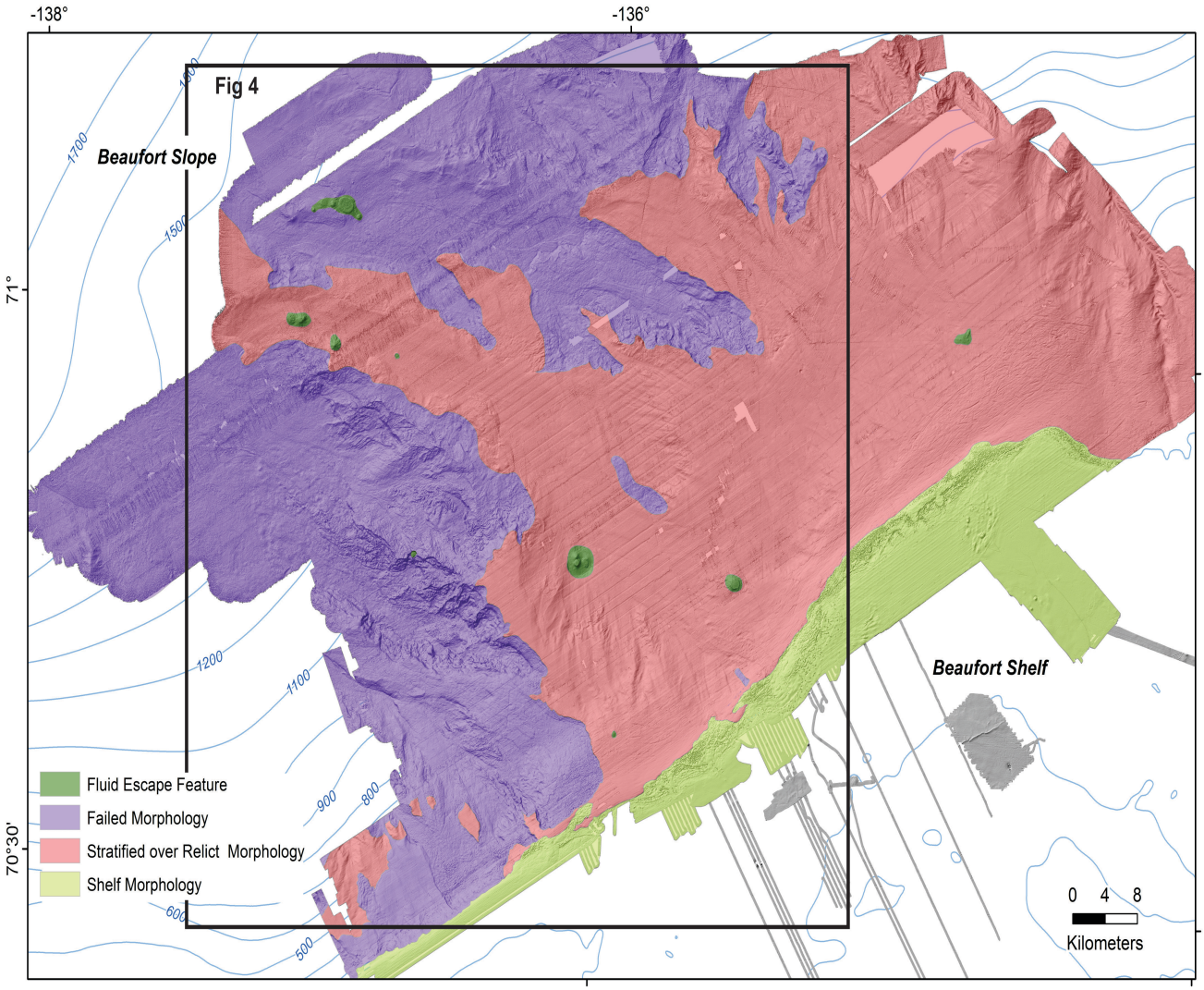

Figure 3. ***Distribution of failed and unfailed sediment with seabed instability features in the Kugmallit Fan study area. Figure location also shown.***

Well stratified fine grained sediment packages, up to 50 m thick, overlie previously eroded and failed morphology, within the unfailed areas (red area, Fig. 3). It is these units which are the "parent"

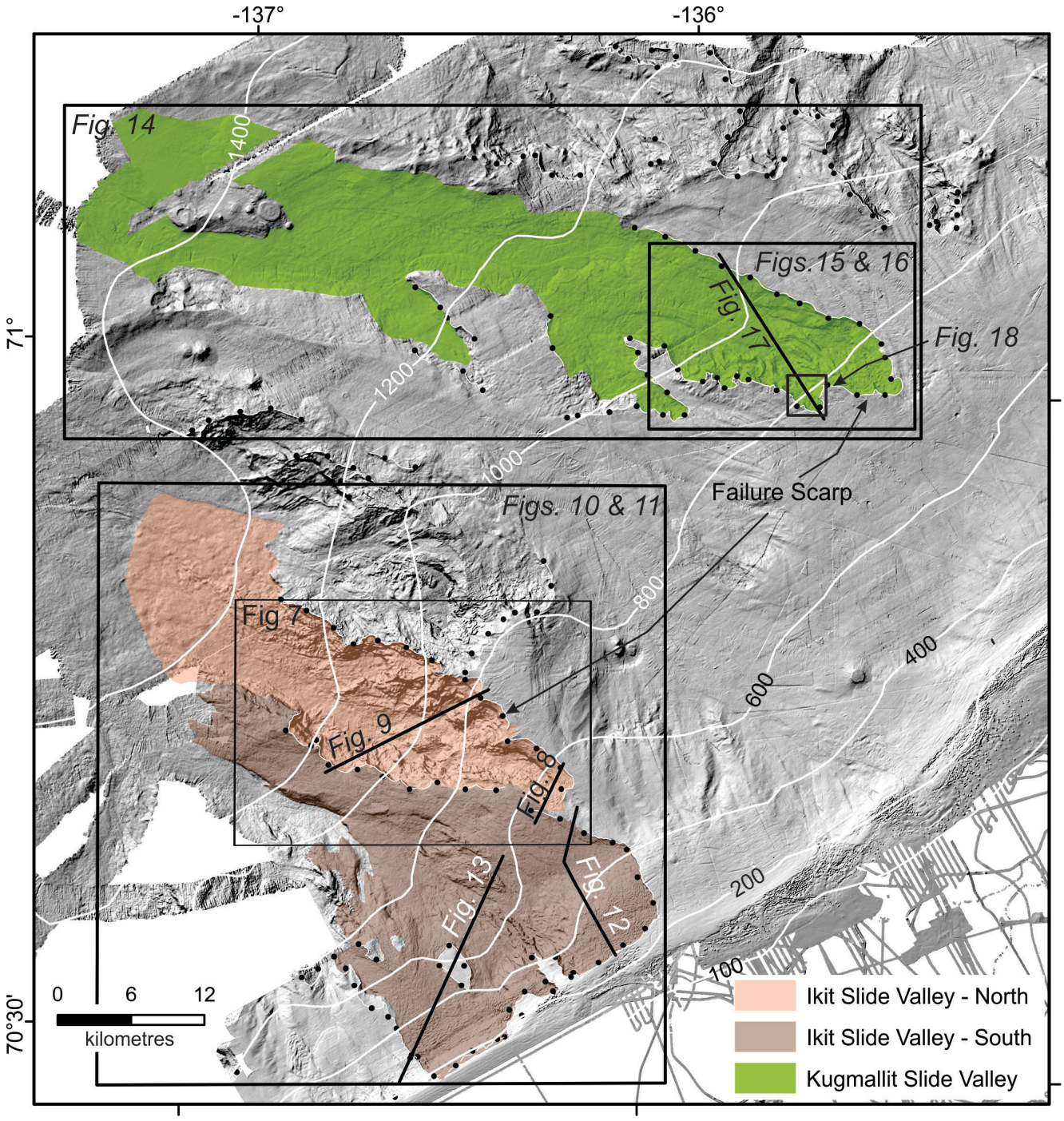

Figure 4. ***Location of Ikit and Kugmallit slide valley complexes, the main focus of this study. Figure locations also shown.***

sediments to the outcropping mass failures. Initial radiocarbon dating of shells and foraminifera in short cores (Blasco et al. 2011 and Woodworth-Lynas et al., 2016), clearly indicates a glacial and post glacial chronology of these parent sediments. Though failure features are recognizable, it is a muted morphology on multibeam imagery whereby the roughness and sharp lineations are partially healed (smoothed) by the mud cover (Figs. 1 and 3). Deformed sediment and numerous failures of fine grained sediment are widespread within the failed morphology (purple area, Fig. 3). Over time-these

multiple failures have created slide valleys on the slope. We separate two distinct slide valleys for detailed morphologic analysis; both whose headwalls extend well upslope (Fig. 4). These are termed the Ikit and Kugmallit slide valley complexes, the Ikit name was introduced by St Ange et al. (2014). Relative age of failure events within Ikit and Kugmallit slide valley complexes is based on cross-cutting and super-position relationships from multibeam and high-resolution seismic profile data. A few small yet young sediment failures are also identified on the map, isolated within the unfailed area, similarly identified by their sharp edges and general "fresh" morphology and their lack of a covering surficial stratified mud layer.

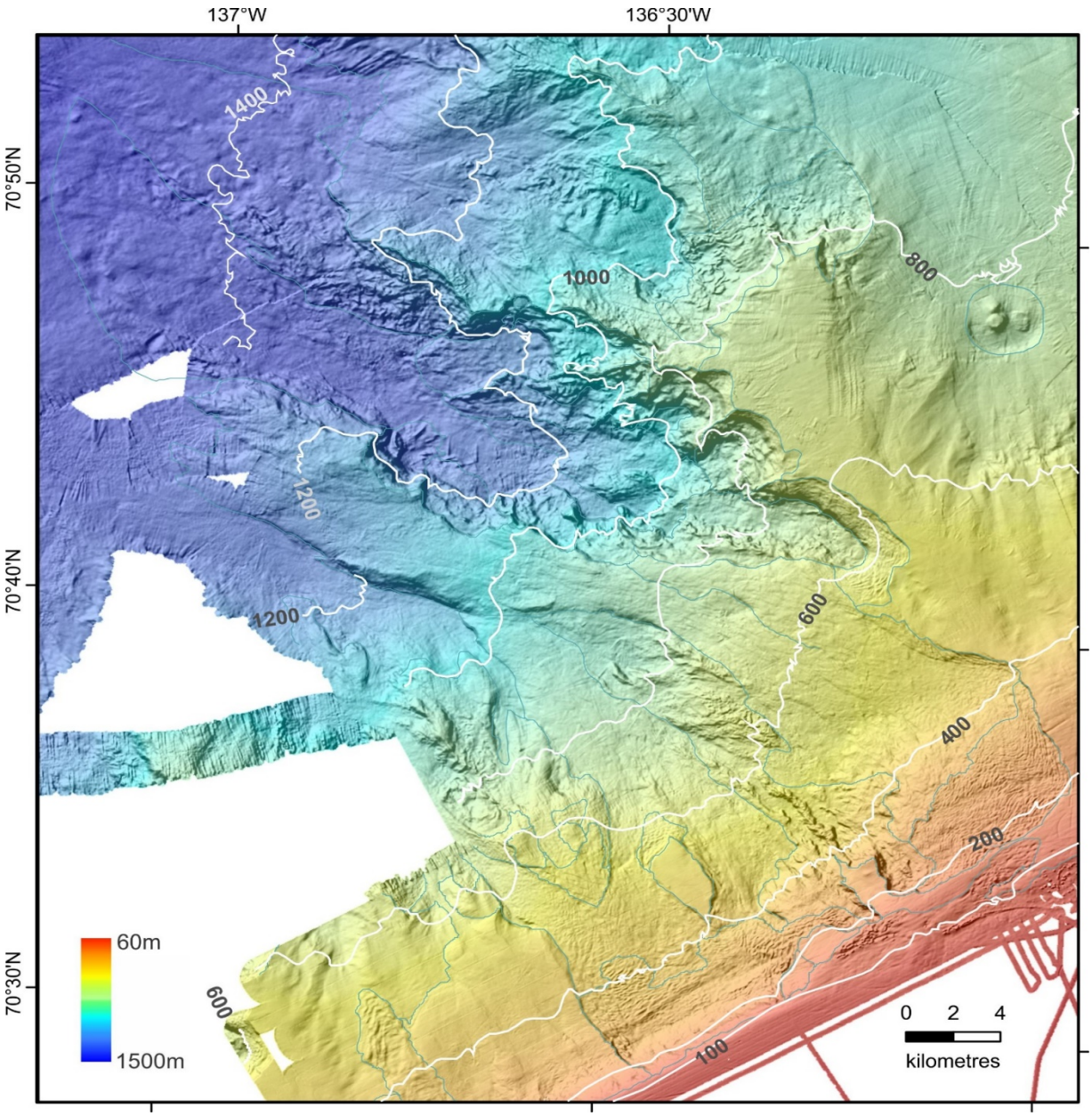

Figure 5. ***Bathymetry of the Ikit Slide Valley Complex. Numerous individual failure events are outlined in faint blue lines and differentiated further in the following illustration. Depth contours (m) smoothed from multibeam data.***

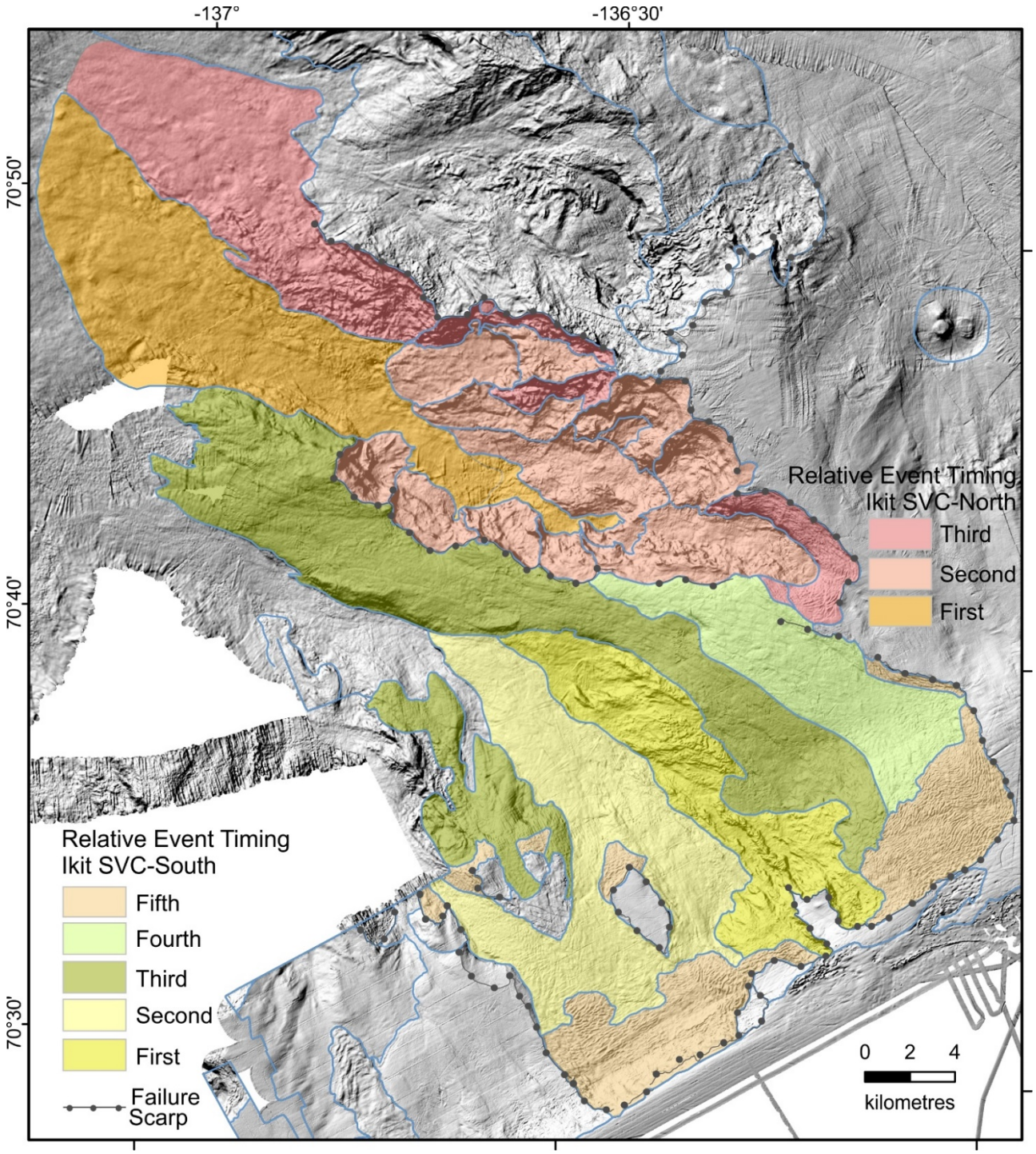

Figure 6. ***Relative timing of sediment failures in the Ikit Slide Valley Complex. Based on cross-cutting relationships, the complex has been subdivided into two areas; South (green and yellow) and North (pink, red and orange). At least five events occurred in the South area and three in the North area. The most recent failures, beige-coloured in the south, include multiple and isolated events. In the north, several contiguous failures are differentiated but not assigned relative timing (light pink) because they are undifferentiable by cross-cutting relationship at this resolution.***

Ikit Slide Valley Complex

The Ikit Slide Valley Complex (SVC) is located on the western Kugmallit Fan (and is about 24 km wide, along the shelf break, extending beyond 55 km (limit of multibeam coverage) downslope, with an area of over 2000 km^2 involving an estimated 45-50 cubic kilometres of failed sediment (excluding unmapped distal portions). Figure 5 shows topographic and bathymetric detail. Rotational and retrogressive failure mechanisms, along with mass transport deposits are identified within the failure complex. Ikit SVC has been subdivided into north and south components, the Ikit SVC-North and Ikit SVC-South, (Fig. 6).

Ikit Slide Valley Complex-North: The Ikit SVC- North is as much as 12 km wide and 41 km long, with an estimated failed sediment volume of 40 cubic kilometres, (Fig 7). Scarp height at the head of the valley can be as high as 220 meters, while the valley deepens downslope to hundreds of meters from the valley flanks. Volumes were estimated using elevations of failure scarps along slide valley perimeters and locations in the valley floor. These estimates are minimums because the topographic divides are generally lower than pre-failure heights and because the base of failed sediment within the valley is rarely imaged on the sub-bottom profiler data.

An irregular, hummocky seabed topography within the slide valley is typical. Rough areas have surface relief features of 10's of metres, are distributed throughout the valley, and can be very blocky. The failed surfaces do not appear draped by post-slide sediment, especially within the third event (Fig. 7). This contrasts with a smoother seabed texture characteristic of some of the MTDs (Figs. 6 and 7, third and fourth Ikit SVC-south). This smooth seabed typically exhibits a downslope-oriented linear fabric and much less relief.

The hummocky rotational failure blocks at the top of the valley have a subparallel, curvilinear pattern that mimics the headscarps (Fig. 7). Unfailed sediments defining the eastern edge of the valley have continuous coherent internal reflectors in seismic profiles (Figs. 8 and 9) and are the parent sediments. These sediments have failed both at the headwall and the sidewall. Correlation of seismic reflectors in the unfailed sediment identifies the stratigraphic level of failures. Seismic profiles also show internal rotational blocks within the curvilinear pattern (Fig. 8).

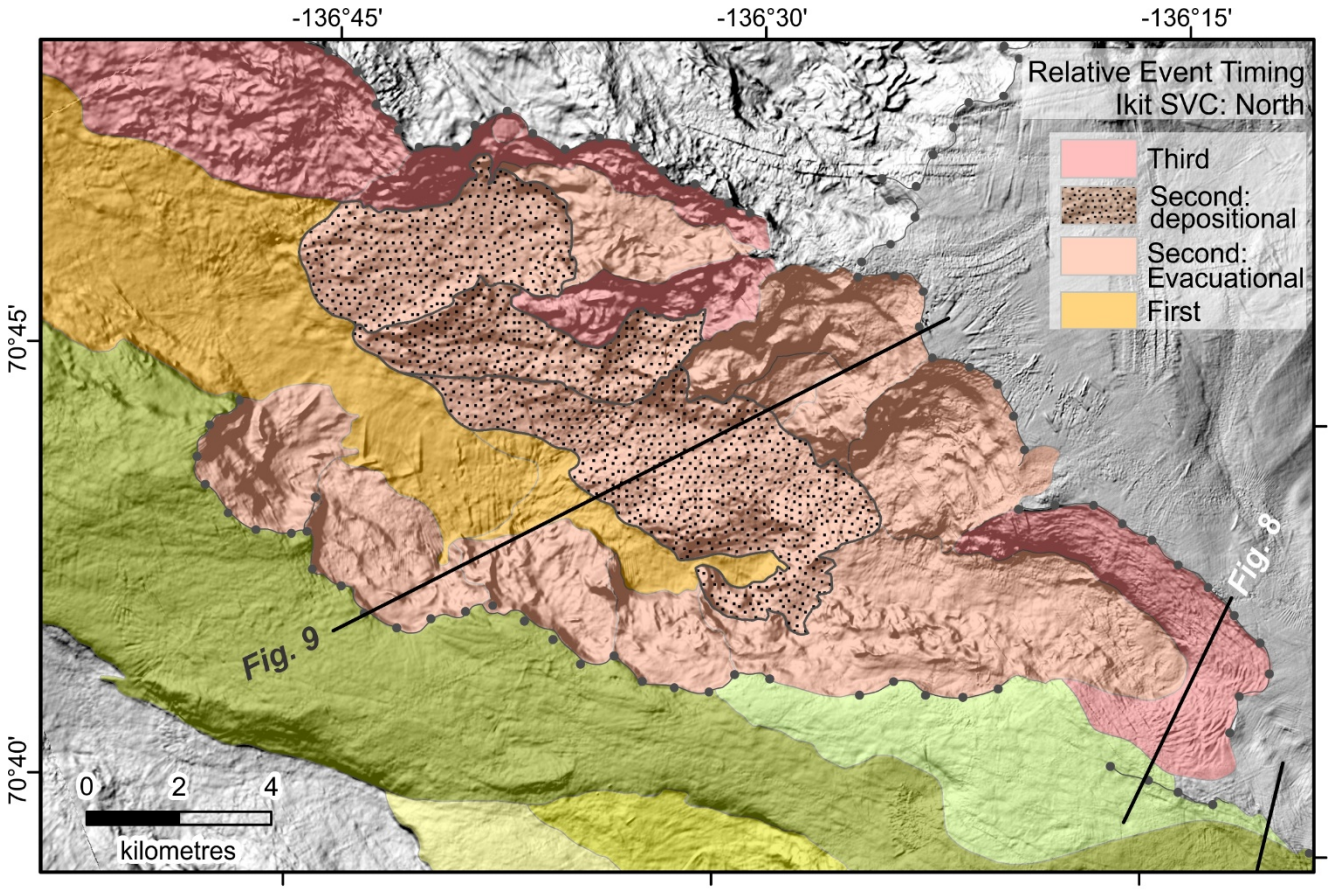

Figure 7. ***Details of Ikit SVC-North successive events. The second event has been differentiated into dominantly evacuational versus depositional areas. Profile illustration locations are also marked. Green and yellow MTDs are Ikit SVC-South which are considered later.***

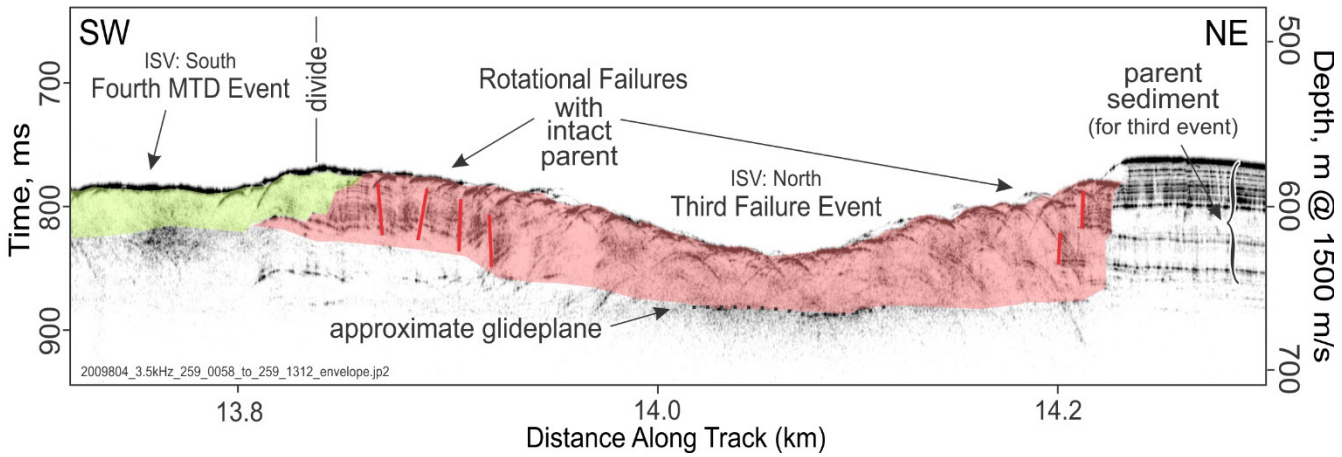

Figure 8. ***3.5 kHz seismic profile (location, Figs.4 and 7) showing internal structure and cross-cutting relationship of failures along profile in the SVC-North. Profile shows a predominant internal rotational style with mostly intact blocks and partly disintegrated masses, giving rise to the arcuate ridge and valley plan view (Fig. 7). The Ikit SVC- South flow (green) is likely pene-contemporaneous or younger than the North valley (pink); while this flowed mainly northwestward in SVC-South, a portion was directed eastward of the divide, into the Ikit SVC-North area.***

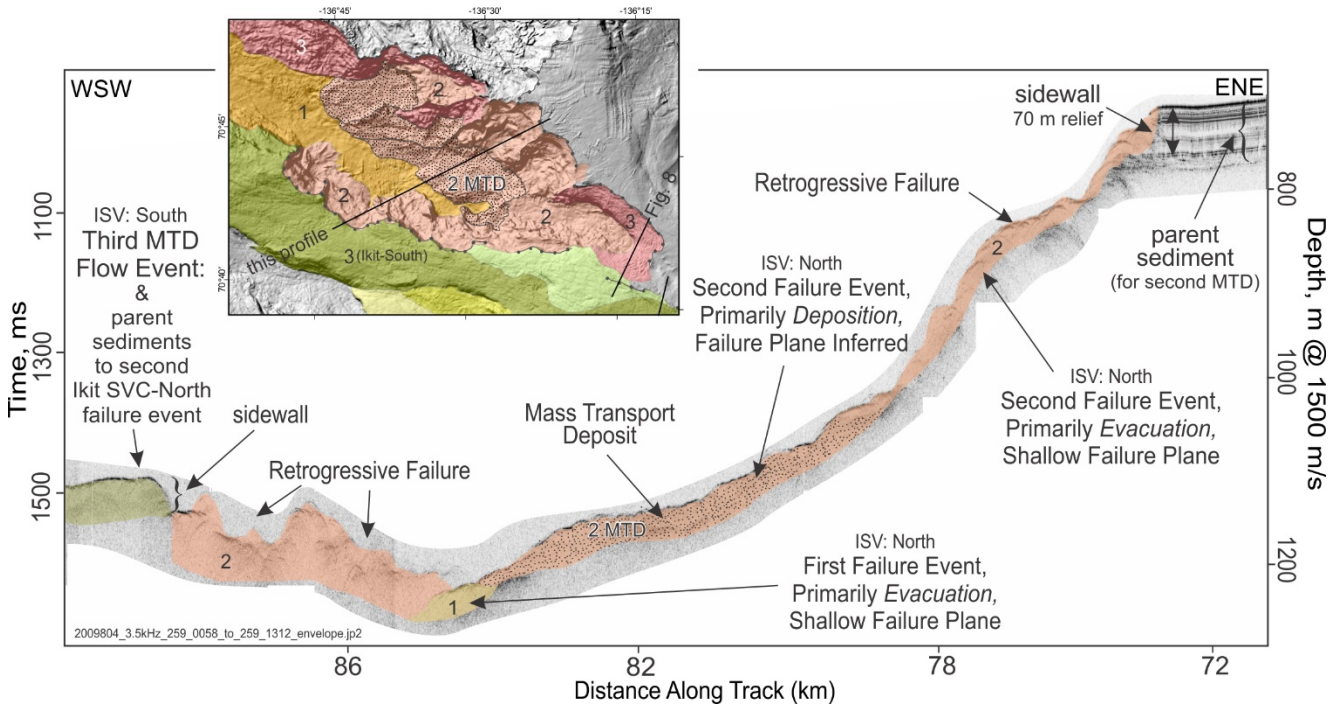

Figure 9. ***3.5 kHz seismic profile (location, Figs. 4 and 7) showing internal structure and cross-cutting relationship of failures in the Ikit SVC-North. Profile shows remobilization in the form of an MTD at the base of the cuspate failure scarps along the north flank, indicating retrogressive failure. We assume some failed deposit also within this scarp, largely unresolved in the sonar data. In contrast, the south flank parent sediments had already failed (part of the Ikit SVC-South) and the cuspate morphology is a later development.***

The orange area in the valley was the first to fail and has since accumulated failed debris from later events. The MTD here exhibits a rough morphology with chaotic internal reflectors on seismic profile, (Fig. 9).

The light pink area in Fig. 7, with the cuspate failures along both flanks of the valley outlines the second main event. The failed sediment partly filling this area is very rough and blocky with chaotic internal reflectors on seismic profile (Fig. 9). These cuspate bowl-shaped failures can be 3-4 kilometres wide and up to 9-10 km in length, with sediment runout flowing beyond that point. These arcuate failures are larger on the north than the south side of the valley, and with much higher scarp walls. They reach up to 14 km^2 with an estimated 0.8 cubic km of sediment evacuated. These failures produced MDTs which overlie the central valley floor MTD confirming their younger age, (Figs. 7 and 9). The cuspate failures on the south side of the Ikit-North valley head in a pre-existing flow-dominated MTD, part of the Ikit-South SVC (Fig. 7). As such this represents a remobilization of sediments that have previously failed.

The side walls of these arcuate failures (red area) have further failed and are especially evident on the northern flank of the valley (Fig. 5 and 7). These smaller failures were amongst the last to occur, probably in response to the new unconfined, over steepened sidewalls.

Ikit Slide Valley Complex-South: The Ikit SVC-South is as much as 22 km wide and 40 km long or more, with bluff heights as much as 20 m (Fig. 10). The estimated evacuated sediment volume is approximately 6-10 cubic kilometres. Based on cross-cutting relationships, a large portion of the complex (green and yellow) is older than the Ikit-North area (pink, red and beige, Fig. 5). Similar to Ikit SVC-North, there are several hummocky areas at the top of the slide area that have a curvilinear pattern, sub-parallel to the headscarps (Fig. 10) suggesting that they are retrogressive rotational landslide blocks

Hummocky areas have relief of 10-20 m (Fig. 10). The principal areas of blocky relief can have a run out from the scarp face of 4.5 km, with a width of 12 km and up to 50 m thick (Figs. 10 and 11). Five successive failure events have been identified in the slide area.

The first failure event exposes a rough and high relief topography with a strong linear fabric oriented up- and down-hill, in the form of erosional remnant ridges and intervening, partly infilled valleys. Though not shown in Fig. 6, both the north and south areas have primarily depositional components filling the distal reaches of the valleys. These extend northwesterly as downslope-elongated and highly mounded deposits with internally chaotic character on sub-bottom profiles. That originating from Ikit-South reaches over 75 m thickness and overlies older failure deposits. From a sediment budget perspective it is likely the equivalent of the first event. It has no discernable sediment cover on the sub-bottom profiles.

The first failure valley (dark yellow) has downlapping failed material originating from both flanks (Fig. 11, light yellow and olive green). The light yellow failure has chaotic and massive internal reflections with intact stratified sediment blocks, while the olive area has a relatively smooth morphology and positive (constructional) relief and overlaps both yellow slide areas, allowing its distinction as the third event. This, in turn is largely conformably overlain by a smaller MTD (Fig. 12), with transparent internal acoustic character, designated the fourth MTD. Finally the beige area has a rough morphology at the seafloor and has rotational failure blocks in seismic section, (Fig. 12). These failures occur within, but mostly at the head of these failure areas and assigned the youngest age. This extends across most of the Ikit SVC-South, generally failing up to the shelf break. The beige failure is not contiguous, separated by an unfailed remnant protruding from the shelf break (Fig. 11) and so a relative age on each components is not possible to discern. A similar unfailed remnant forms an "island" intersected by the Fig. 13 profile.

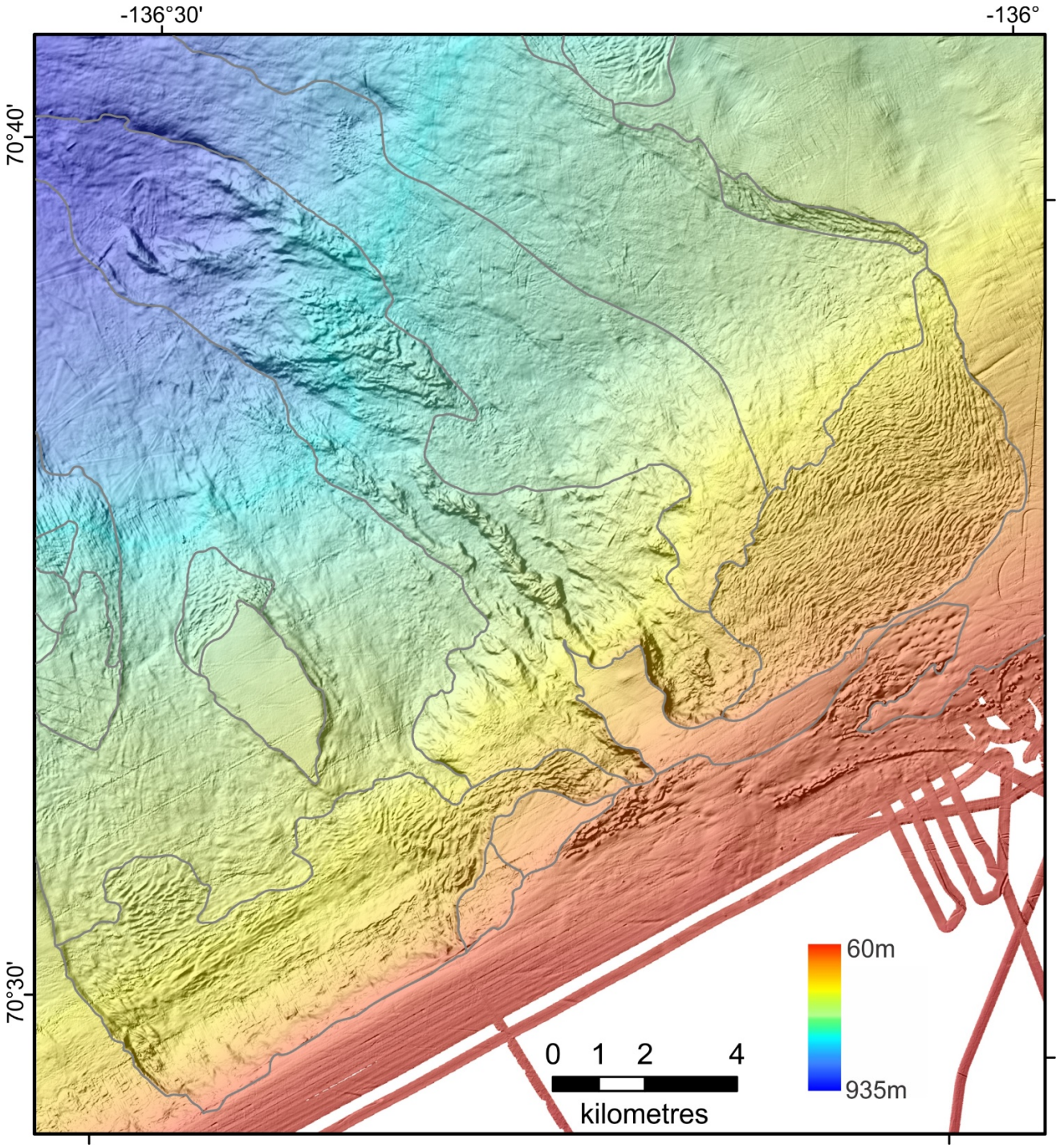

Figure 10. ***Topography and bathymetry of the upper reaches of Ikit SVC-South. Grey lines outline sub-divisions shown in the following illustration. The ribbed pattern is most common adjacent the headwalls and is a retrogressive rotational style. The central zone, displaying the roughest and more down-slope oriented ridge and valley topography, cut deep into underlying stratigraphy. Much of the topography is thought to mimic the basal failure plane though blocky deposits overlying this are common. The flanking MTDs exhibit more down-hill flowlines.***

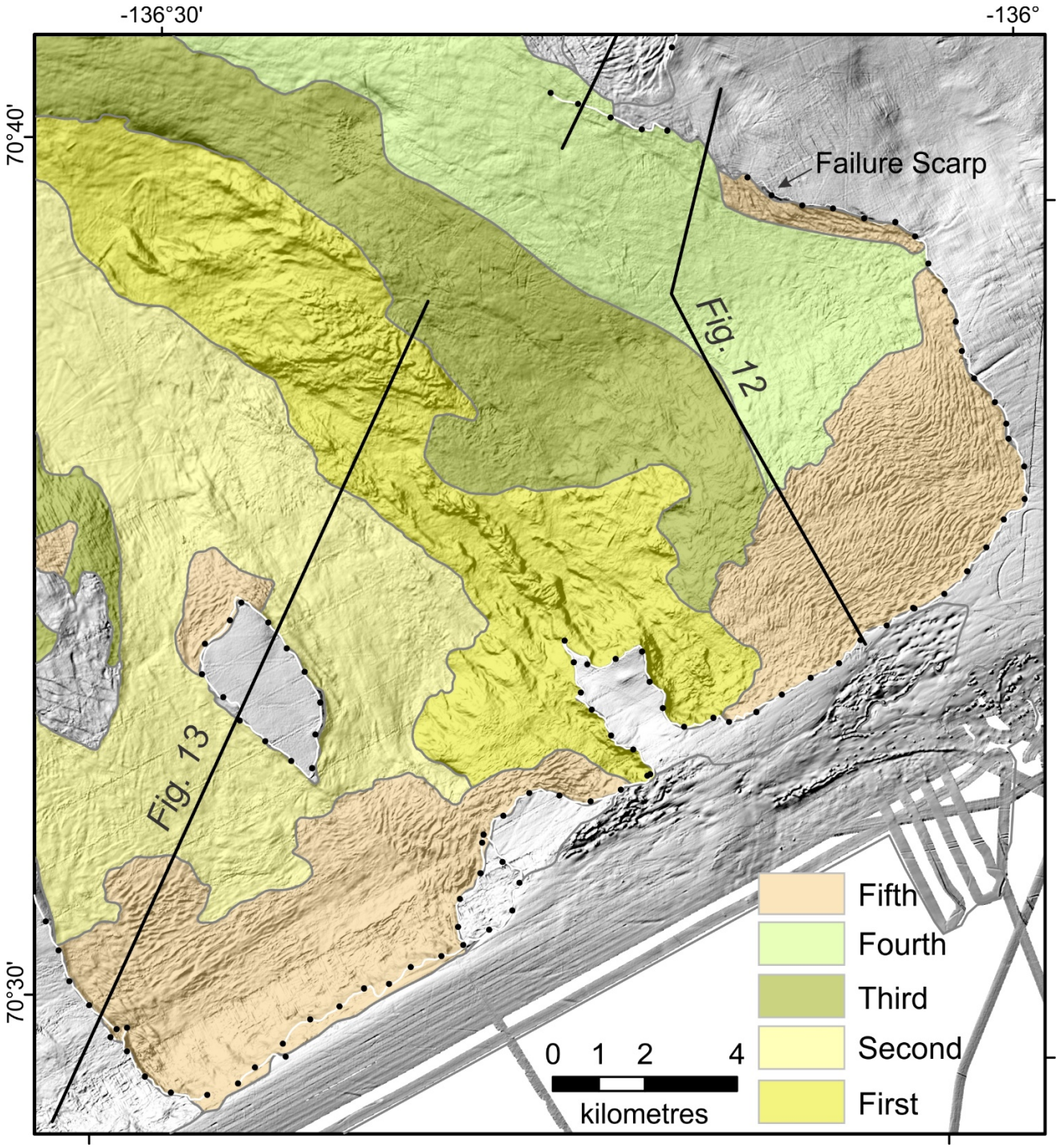

Figure 11. ***In the upper reaches of the Ikit SVC-South five failure events are differentiated; the first evacuated to the deepest stratigraphic levels and the second and third flank the original valley As discussed in the text, relative timing of non-contiguous failure elements is largely precluded such that the difference in timing of the two events (beige and yellow on this profile) may be very close. Accordingly, the third and fourth events need not have intervened.***

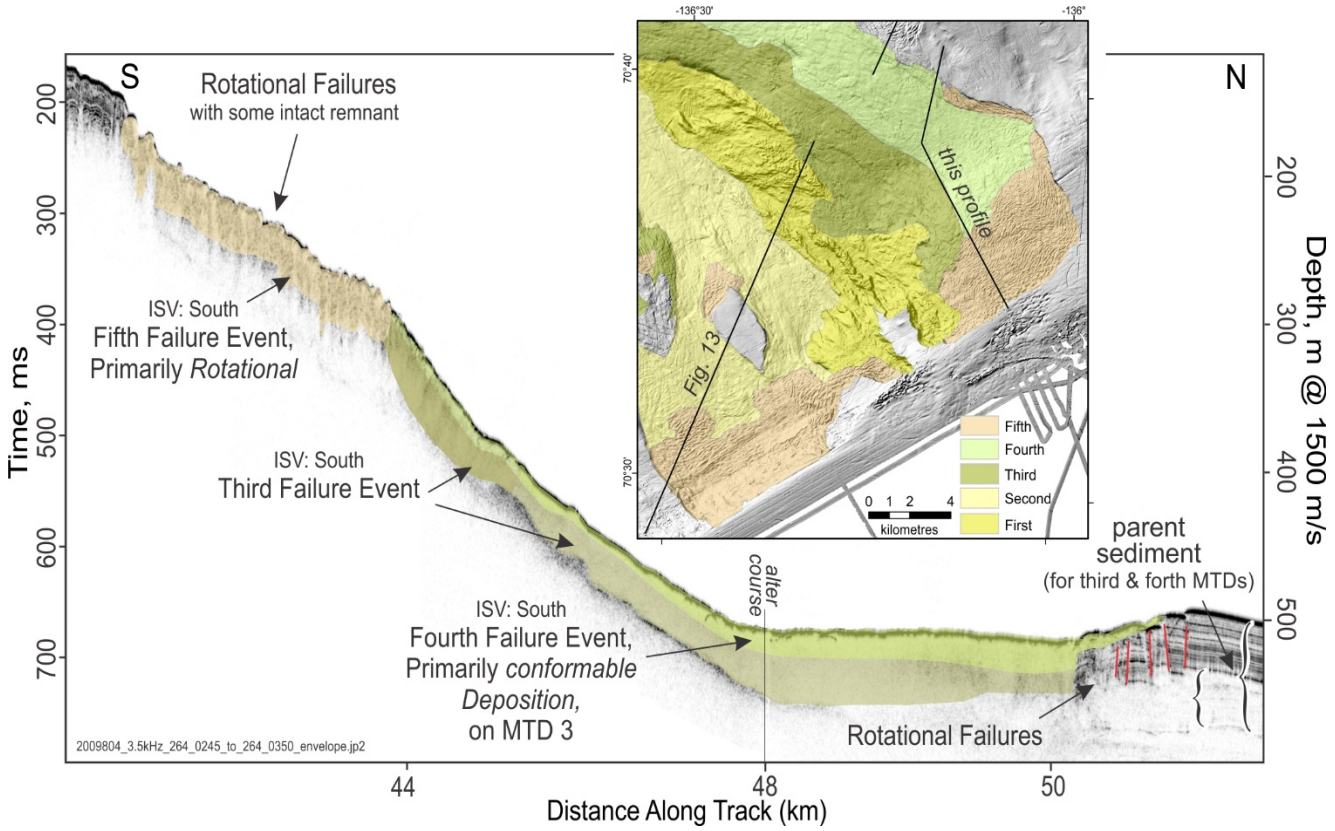

Figure 12. ***Map and 3.5 kHz seismic profile (location also on Fig. 4), showing internal structure and cross-cutting relationship of failures along profile in the ISA: South. The fourth event MTD (light green) overlies the thicker third (olive) yet the fifth (beige) apparently abuts the previous MTDs. Only the third MDT seems to have involved the lower half of parent sediments (brackets, right), below the well stratified horizons; the others mobilized the upper half.***

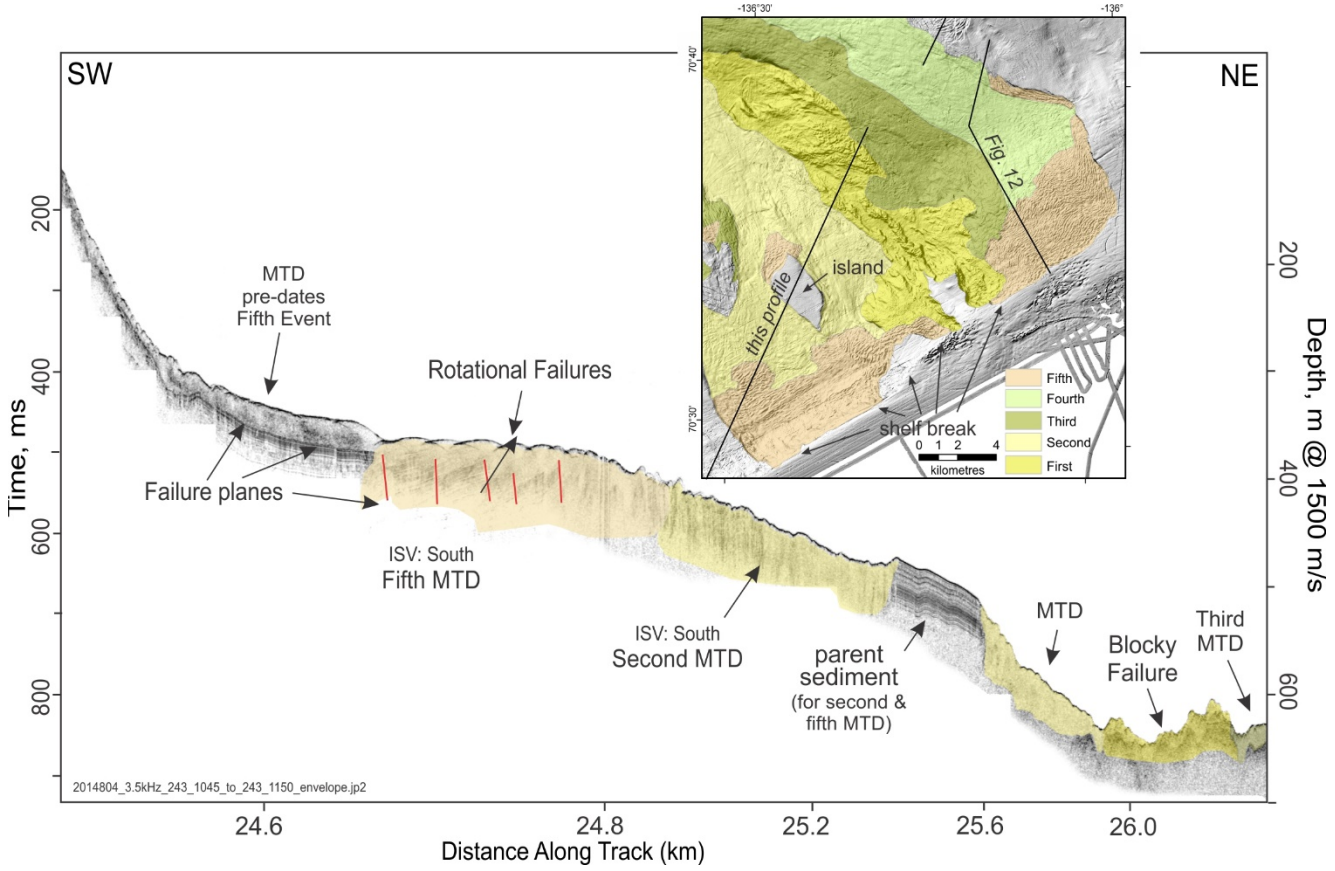

Figure 13. ***Another profile across Ikit SVC: South. This transects the initial failure (dark yellow) which has left only blocky remnants in a primarily evacuation zone. The following event (light yellow) likely only translated short distance because remnants of the original stratigraphy are intact. It contrasts, however, with the fifth (beige) MTD where original parent stratification is largely intact, having only rotated in segments, initially abutting the earlier (light yellow) MTD and progressing up-slope. The beige failure plane is deeper than an earlier event (left, uncoloured) and the marked sidewall (bottom leftmost on the map) depicts a net evacuation here of the fifth and second events. The unfailed "island" is a rare occurrence but has analogues in the intact remnants still adjoining the shelf break.***

Kugmallit Slide Valley Complex

The Kugmallit SVC is located in the north central part of KF, (Figs. 4 and 14) and extends at least 68 km down-slope and 14 km wide, with an area of approximately 1535 km^2. A volume estimate suffers the same limitations as at Ikit SVC, with unmeasured thalweg fill and unknown amount of translation out of the map area. Nevertheless, at least 100 km^3 was removed. At the top of the failure complex, the headscarp can be over 40 m high. On the northeastern flank of the complex the failure scar can be over 70 m to the failure floor.

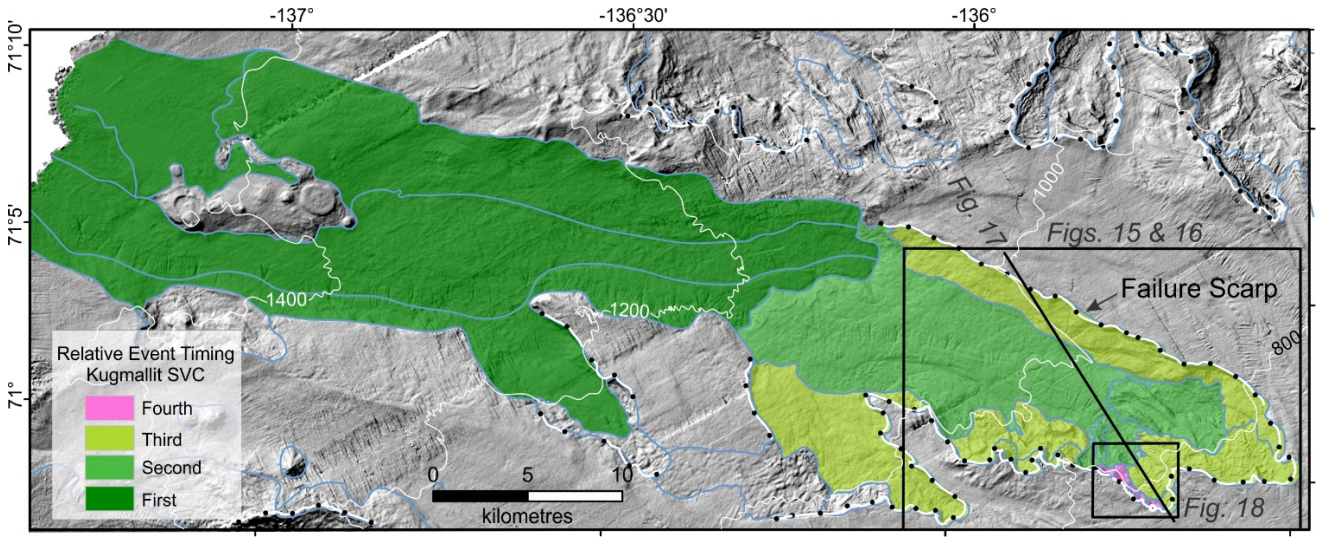

Figure 14. R*elative timing (first to forth) of sediment failures in Kugmallit SVC. Additional failure events are outlined in grey- blue lines but their relative age is not well defined. These slides may be similar in age to those found in the Ikit SVC.*

Lower Reaches: The Kugmallit SVC presents a deep initial failure in its lower reaches, similar to the Ikit SVC, with net evacuation and sediment bypass. The seafloor here is moderately rough except in the center of the failure complex where the MTD has relatively smooth linear ridge morphology and low relief and a dominantly transparent acoustic character. Sub-bottom profiler data from downhill, beyond the multibeam coverage (not illustrated), indicate a thick depositional body. This is a long run-out through a depositional tongue fed by the central axially-oriented flow-dominated component (Fig. 14). Its southern flank has a tributary valley but otherwise little of the cuspate rotational failure of the Ikit SVC. Here, the flanks preserve depositional aprons representing axial-normal failure but without much subsequent retrogression. These aprons do not present a clear timing relationship with the central (axial) flow.

Upper Reaches: The topography of the upper Kugmallit SVC reaches shows variable topography where numerous failures have been identified (Fig. 15). The initial event (dark green in Fig.14) was followed by a second axially-oriented evacuation with a dominant flow character except at its headwall (Fig. 16) where at least two near synchronous events have an evacuation-dominated topography. A tributary valley and numerous small arcuate retrogressive failures occur along the southern flank in the upper reaches of the slide complex, (Figs. 15 and 16). These arcuate failures can be as much as 1-2 kilometres wide and up to 2-3 km in length, with sediment runout flowing beyond that point. Retrogressive sediment ridge blocks, parallel to the scarp face, characterize the floor of these arcuate failures.

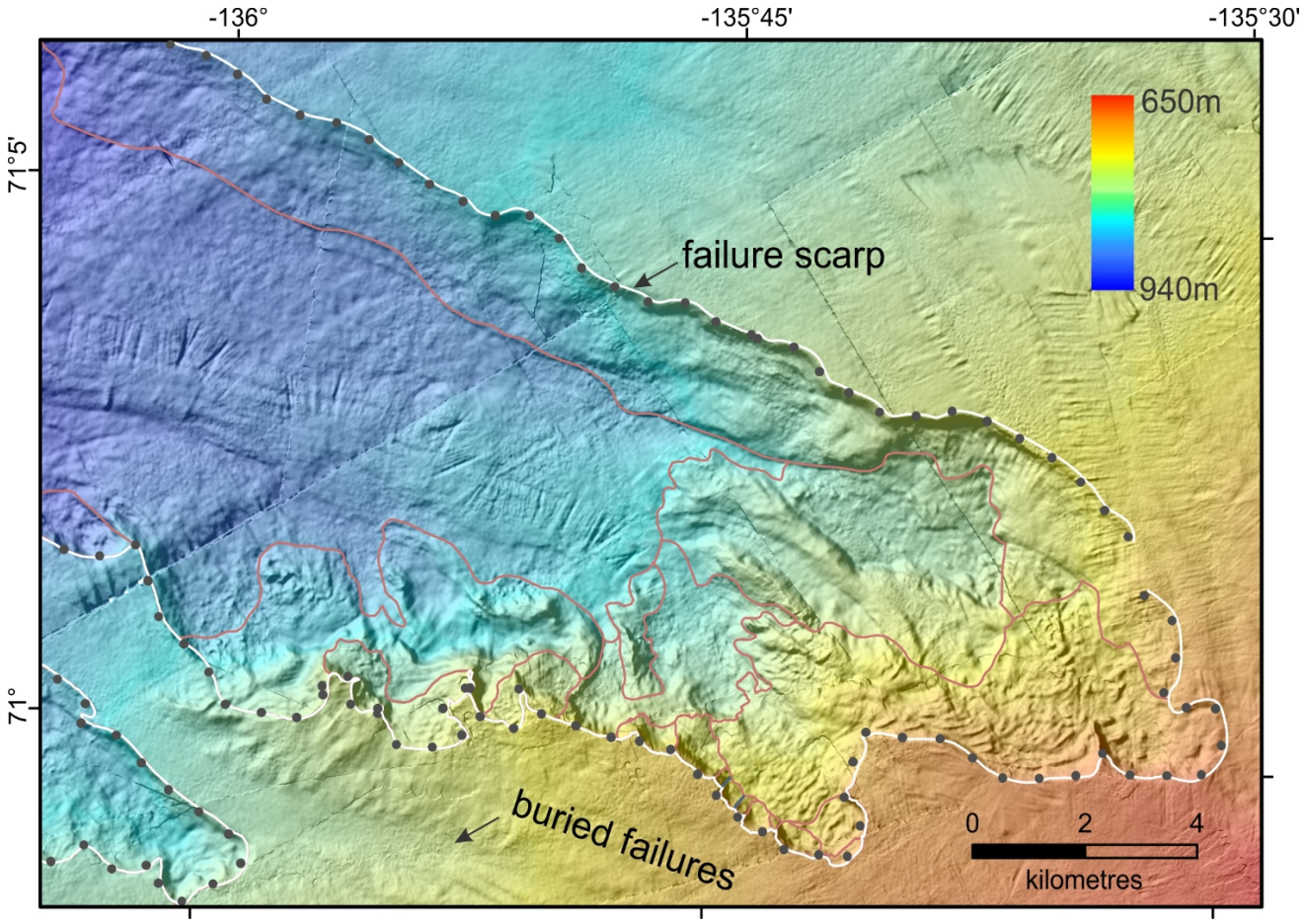

Figure 15 ***Topography and bathymetry of the upper reaches of Kugmallit SVC. Brown lines outline other failure subdivisions whose timing is less clear. The central zone is relatively smooth and with downslope-oriented flowlines. Cuspate bowl-shaped failures with blocky ridge and valley morphology ring this headscarp but are more prevalent and numerous on the uphill flank. Older, buried slide scars are mimicked below between 10 and 30 m of undisturbed late and post-glacial mud immediately south of the southern headwall.***

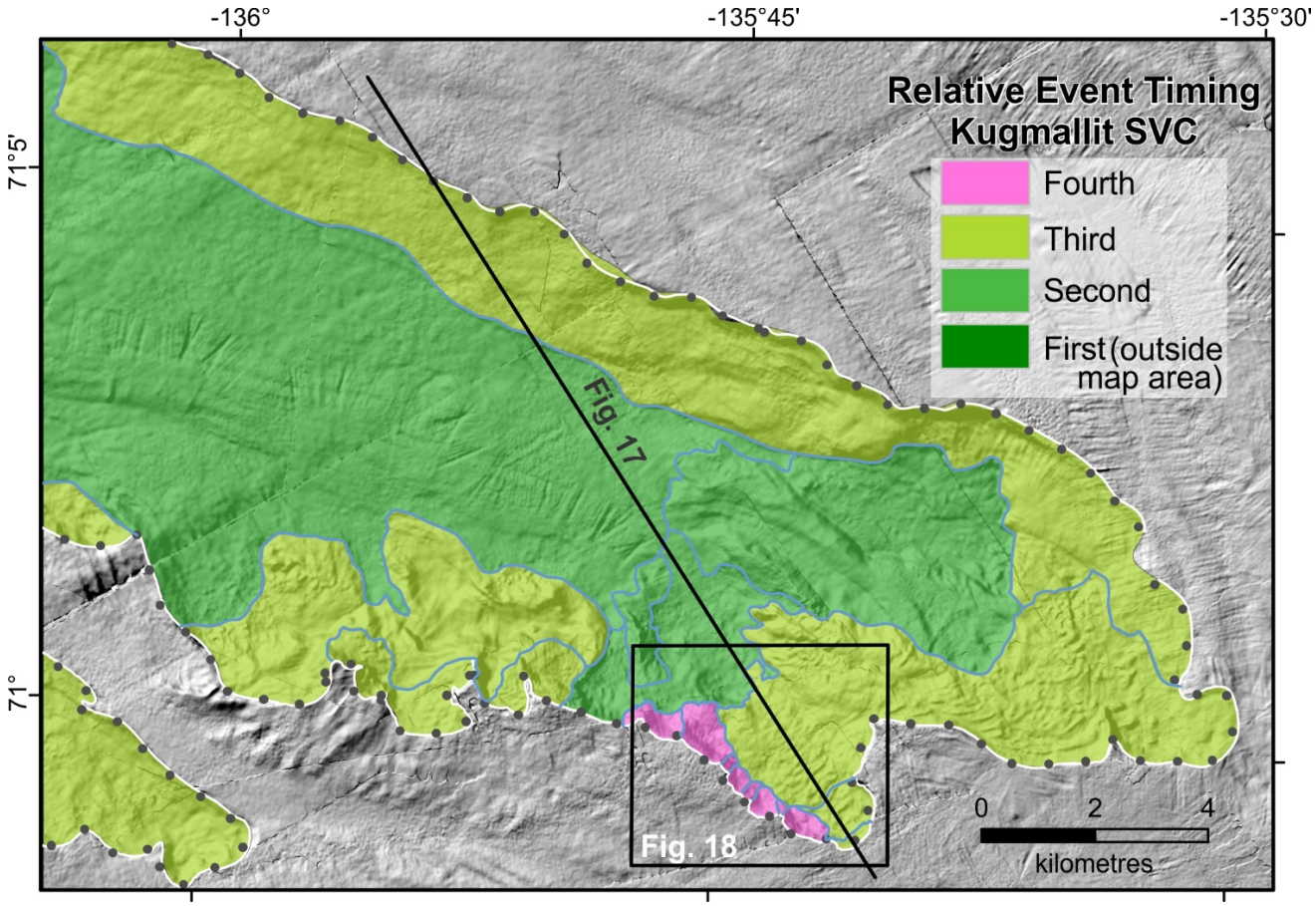

Figure 16. ***Individual failure entities constitute different styles (light green) outlined by the blue-grey lines. The transition from evacuation to deposition is marked by the grey line across the second (mid-tone green) slide event. Timing for many of the cuspate retrogressive events cannot be discerned (light green and pink) despite their contiguity. The most recent failures (pink) indicate a progressive and continued retrogressive failure. Profile and high resolution map locations are shown.***

Seismic profile data show a hummocky seafloor with internal rotational blocks and chaotic reflector at the head of the valley and along the flanks of the slide complex, (Fig. 17). The rotational failures can be up to 50 m thick and pinch-out basinward. The sediment blocks rotate with decollement at the base of the stratified section. The profiles also demonstrate a superposition on the basinward limit of the deposits, indicating that these head and sidewall failures post-date the main (central) evacuation and flow.

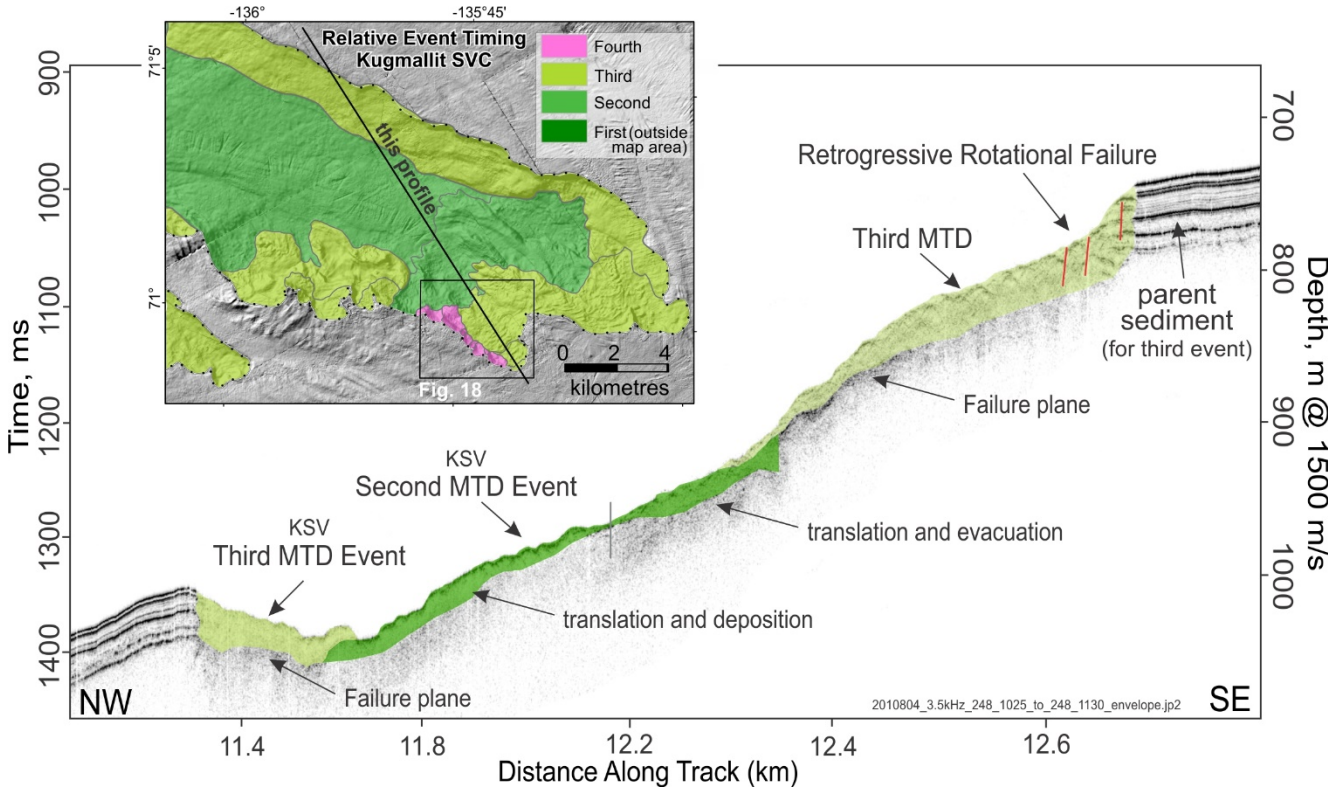

Figure 17. ***Location and profile across the upper reaches of KSC. The lower failure plane is well imaged at the base of the third MTD (light green) which has a strong retrogressive component. These overlie pre-existing mass transport deposits (darker green) deeper in the valley. Within the dark green failure, a primarily evacuational component in the upper reaches is differentiated from a primarily depositonal MTD body, the boundary represented by the grey vertical line in profile and the blue-grey line in Figure 16. The light green failures (third) overly the dark (second) and involve the full thickness of the stratified parent sediment blanket.***

The uppermost Kugmallit SVC reaches were surveyed with an Autonomous Underwater Vehicle (AUV) equipped with multibeam and CHIRP sonar (Melling et al. 2013). The additional resolution afforded by a 50 m survey height allows enhanced recognition of process and cross-cutting (Fig. 18). Cuspate head- and sidewalls, rotational and translated blocks, near fully disintegrated flow in conduits, and several generations of retrogressive activity are all elements clearly identified.

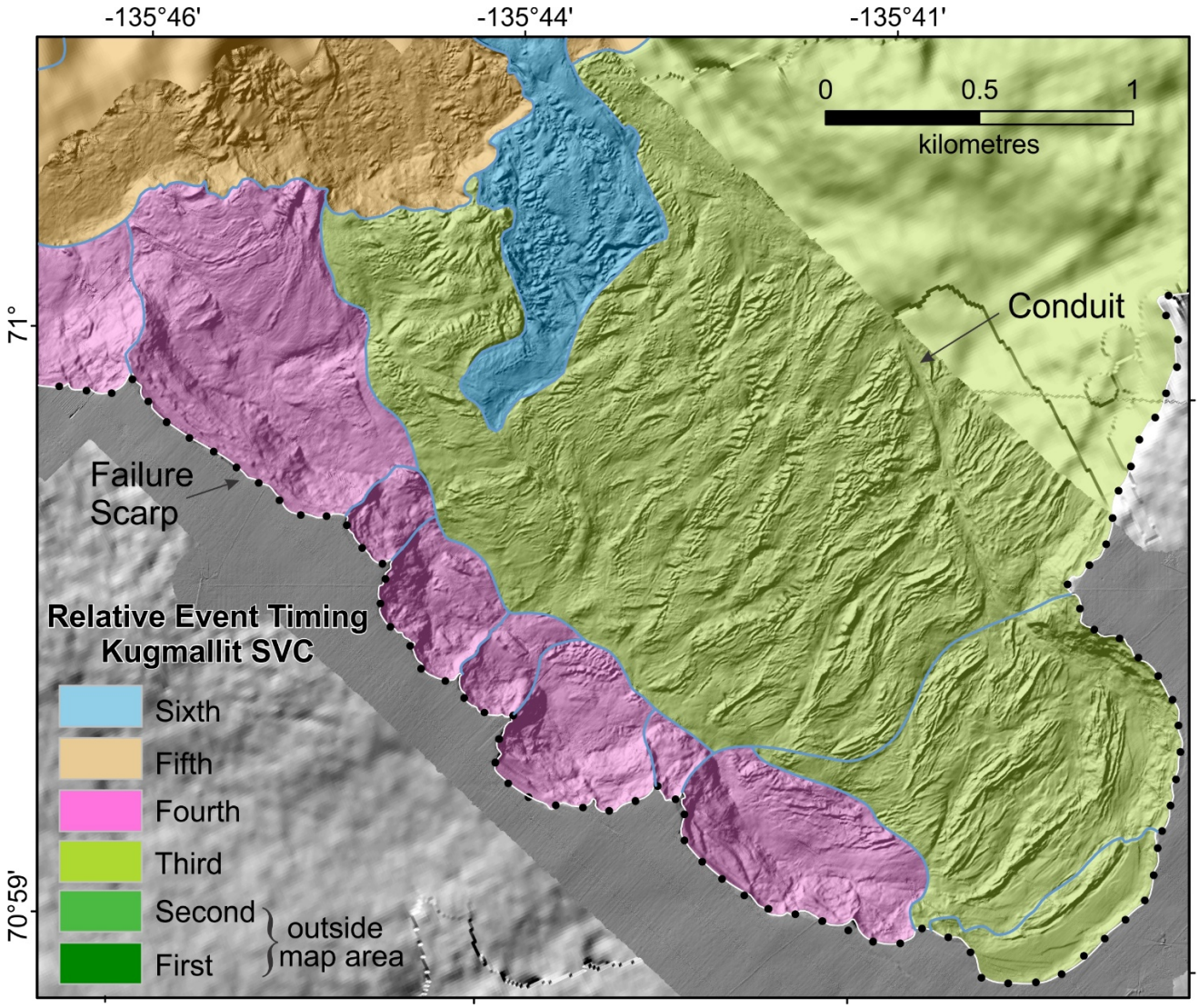

Figure 18. Detailed map at the head of the Kugmallit SVC where high resolution AUV multibeam imagery collected and processed by the Monterey Bay Research Aquarium. This shows deformed ridge and valley morphology of rotational and translated blocks, each with smaller scale ridges. The cuspate bowl failures on the southern face (pink) failure events followed. Their deposits include both blocky rotation and flow which overrides the main (third) event (light green). This failed yet again repeatedly (orange, then blue), the latter probably due to oversteepening at the new headscarp. Both blocks and disintegrated material remain. Note the fully disintegrated flow, labelled "conduit" originating from the headscarp within the third (green) failure. Similarly, the blue area flowed in the lowermost region, breaching the scarp and spreading across the orange MTD. Location, Figs. 4, 14 and 16.

Summary and evolution of the Ikit and Kugmallit slide complexes

The central and deep areas of both Ikit North and Ikit-South complexes (dark yellow and orange, Fig. 6) were the first and the stratigraphically deepest to fail. The valley thalweg was left with rough, high relief and locally blocky and linear ridge morphology. This presented steep and now unconfined head- and sidewall faces, clearly over steepened and subject to further failure. Runout for both complexes is represented by thick flows out of the study area. This too was followed by side and headwall MTDs that have largely accumulated within the first evacuation area.

The boundary between Ikit-North and Ikit-South is largely represented by removal of the third and fourth events in the south by the third event in the north (Figs. 6 to 9, where red cuts greens). Thus, the northern complex is younger than the southern. This second set of the Ikit-North valley flank retrogressive failures widened the valley in places by nearly 9 km. The larger of these are arcuate failures occur along the northern valley flank. The sediment from these accumulated mainly in the new valley thalweg, creating a very rough, blocky and hummocky morphology overlying the first failure (Figs. 6 to 9). Similarly, at Kugmallit, the third and fourth failures events occurred after most of the sediment had been evacuated from the slide area, allowing the unconfined sediments along the scarps to fail.

Across the whole Kugmallit SVC, no post-failure sedimentation is recognized in sub-bottom profiler data, in likeness with the Ikit SVC, suggesting relatively recent and possibly synchronous activity. In cores the post-failure sedimentation appears to be consistently only decimetres or less thick and a recent and possibly similar age for both complexes is suggested (Cameron, et al. 2017).

Sediment Re-failure: The cross-cutting contact between Ikit-North and Ikit-South failure events represents a remobilization of previously failed sediment (Figs. 7 and 9, red cutting olive green). This is despite dewatering, stiffening, and slope-flattening of the earlier flow (olive green), all factors that contribute to the original failed and transported mass finally coming to rest. Apparently the flow can retain some of the original instability properties only to fail again where slope oversteepening redeveloped through these bowl-shaped retrogressive failures. This may be an indicator that so little time elapsed between subsequent failures that dewatering had not progressed, that a second (seismic?) trigger occurred, or that the increased loading from the flow emplacement de-stabilized its underlying foundation.

Absolute age of the Mass Failures

Determining the absolute age of the slides in general and that of the individual events presents significant challenges. The approach has been multi-faceted and includes seismic superposition and cross-cutting relationships presented here, and sampling of the post-slide mud cover (if present), its sedimentological recognition, and then it's dating. Both C-14 and Cs/Pb techniques have been utilized (Cameron et al. 2017).

From a sub-bottom profiler viewpoint the approach has been to first understand the present day sedimentation setting of the Holocene Mackenzie River derived muds. The adjacent shelf break demonstrates a highly variable mud distribution with both depositional and erosional elements (King et al. 2017). They tie seismic horizons to an assembly of C-14 dated cores, largely unpublished except for that of Bringué, and Rochon (2012). King, (2017) demonstrated that uppermost slope Holocene age muds, though largely bypassing the shelf break, can reach many metres thickness immediately beyond the shelf-break where oceanographic conditions diminish and allow rainout. They also confirmed a linear sedimentation rate spanning the mid Holocene to present, demonstrated in the

Bringué, and Rochon work. Accordingly, a mud cover so thin as to be unresolved on the 3.5kHz profiles, as demonstrated on Kugmallit and Ikit SVCs, would only span a portion of the late Holocene. Furthermore, the head and sidewalls clearly cut the entirety of this parent material to horizons within the resolution of the profiler data, at least sub-metre, likely better than 1/3 m. In terms of age, this translates to the last millennia or less, given linear sedimentation rates just beyond the shelf-break.

The other slide age dating approach is by recognition and dating of the overlying blanket from cores and box cores. This has been performed with some success (Cameron et al. 2017) but uncertainties remain. Such interpretation of dating results relies on the ability to identify the top of slide material through differentiating post-slide from slide-translated parent sediments. This is problematic where the translated material is largely undisturbed, as in the retrogressive rotational zones. Nevertheless they suggest that the latest mass failure activity is less than 1000yr. Further work is addressing the dating repeatability on different slide segments and the sedimentological differentiation of the cover and parent.

FAILURE MECHANISMS

The KF has numerous, large sediment failure complexes on the Beaufort Slope. These failure complexes are part of a larger system of submarine canyon and valley morphology on the Beaufort Slope, (Fig. 19). Based on crosscutting relationships and morphology, there have been numerous sediment slides identified within each slide complex. In assessing the cause of landsliding, it is important to distinguish preconditioning factors and triggers.

Failure-susceptible horizons

Failure plans have been recognized at the base of rotation in the upper retrogressive arcuate ridge and valley terrains (e.g. third MTD in Ikit SVC-South, Fig. 8) or where cover material is thin enough to image an underling reflector (e.g. Ikit SVC-South, first MTD, Fig. 13). Typically this is not planar but ridged and canyoned. Clearly, the valleys cut in the initial event are not planar but “V”-formed, like large canyons. Accordingly, a typical translational movement is not generally recognized.

However, typical of the third and fourth failure events is that they involve previously undisturbed, stratified parent sediments comprising two stratigraphic units recognized on the sub-bottom profiler data; an uppermost, well stratified unit and a lower, poorly stratified unit (see parent sediment designations in profile Figs. 9, 12 and 13). These are deglacial and post-glacial muds where initial age dating compilation shows exponentially diminishing sedimentation rates (King, pers. comm. based largely on C-14 ages in Woodworth-Lynas et al., (2016).

Though there are exceptions, the retrogressive activity reaches down to the base of these two units, notably not involving the more acoustically impenetrable (harder?) surface below them. Furthermore, with sediment movement and further translation, the lower (less well stratified) portion progressively disintegrates (seismically), manifest as a loss in volume and loss of continuity in strata, while the overlying (well stratified) unit maintains its integrity, generally “riding” the block further downhill.

Eventually, even this upper unit disintegrates. One interpretation is a greater failure susceptibility of the lower unit. Part of this is simply due to the greater sediment load (depth of burial) but the lower unit responds as a whole (its entire thickness) suggesting that some inherent property of the unit is responsible for its behavior. There is limited evidence for a lower consolidation in the lower portions of the deepest core material sampled (MacKillop et al. 2015). This is in contrast to normal consolidation in the upper units. The high sedimentation rate in the lower sediment package, noted above, may be reflected in diminished de-watering of the lower unit and, with subsequent loading, increased porewater pressures.

Fluids and Sediment Pre-conditioning

Shallow gas and fluids are important pre-conditioning factors, in permeable marine sediment, in subsea failures, (cf. Piper et al. 1999; Lafuerza et al. 2012, Winkelmann and Stein 2007, Krastel et al. 2016). Shallow gas occurs in many areas within the Beaufort Sea, (Blasco et al. 2011). Evidence for fluid escape is widespread at the seafloor in KF: Numerous fluid escape features, such as mud volcanoes exist on the slope, and hundreds of pingo-like features occur along the shelf break, (Fig. 3). Paull, et al. (2007, 2011 and 2015a, 2015b) report on shelf edge and Beaufort slope fluid escape features and attributed these features to on-going melting of permafrost, gas hydrate or venting of methane. Fluid escape features in the form of slope-situated mud volcanoes are briefly described in Saint-Ange, et al. (2014) and in Woodworth-Lynas, et al. (2016). Characterization in terms of process and activity comes from two mud volcanoes that have been the subject of intense study (Jin et al. 2015, Paull et al. 2015a, DongHun et al. 2016). Continued studies of mud volcanoes, include 2016 and 2017 field activities, investigations of activity levels and flow patterns from repeat AUV surveys, core sampling, temperature and heat flow, porewater geochemistry, and biomarkers (Melling et al. 2013, Jin, et al., 2018.).

The PLFs on the shelf occur likely as the result of upward extrusion of sediment under pressure from escaping gas through overlying weaknesses in sub-seafloor permafrost. Paull et al. (2007, 2011, 2015b) described anomalies in seismic profiles consistent with free-phase gas in the sediment. St. Ange et al. (2014) identified more than 40 active gas vents at the shelf break and upper slope in the ISA and entertained the idea of a possible connection with slope failures. Riedel et al. (2015) further identified deep-seated free gas and bottom-simulating reflectors (BSRs), indicative of hydrate stability. In a decaying outer shelf permafrost scenario (Paull et al. 2007, 2011) dissociation of such hydrates is a potential source for such seabed gas release. If pathways for fluids are partly from these types of features and partly through impermeable strata, then the Beaufort Slope will probably have higher pore pressures, which is an important pre-condition for sediment failure.

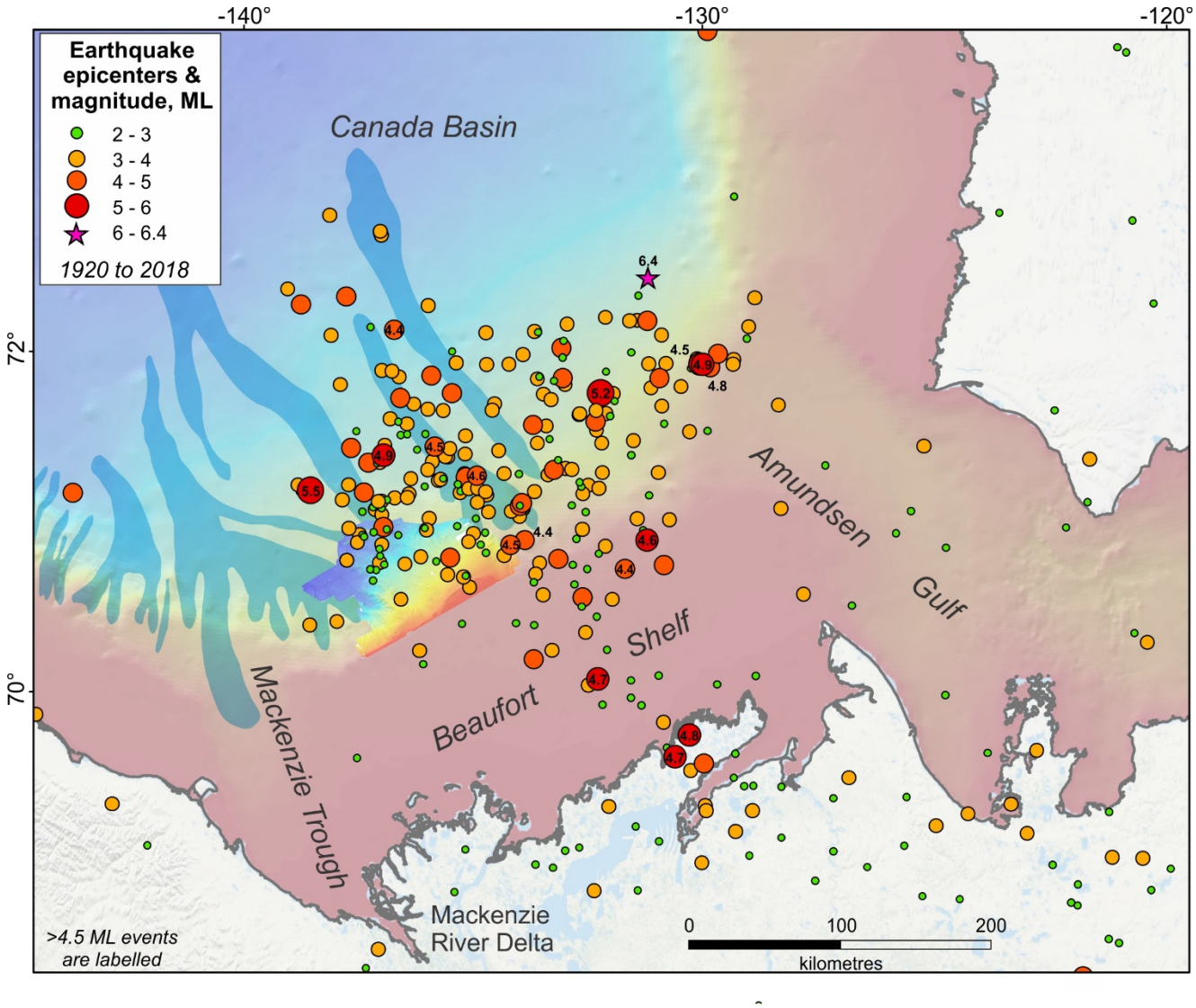

Figure 19. ***Historical earthquake epicentre distribution shows high seismic activity between 1920 and 2018 in the southern Beaufort Sea and within KF (black outline). Red areas within the KF are multiple failure event valleys. Blue areas are slide valleys or canyons (highly generalized) and show that the KSC's are part of a larger system of submarine canyon and valley morphology on the Beaufort Slope (from Harris et al. 2014). Earthquake epicenter data is from Halchuk, et al. (2015) and http://www.earthquakescanada.nrcan.gc.ca/. Note the 6.4 MN off Amundsen Gulf (purple star, 1920 event).***

Seismicity

The southern Beaufort Sea is seismically active, within historical times, with minor to strong earthquakes mostly concentrated on the Beaufort slope near and within the KF, (Fig. 19). There is approximately one earthquake of M > 4 per year, and one M > 5 expected roughly every 10 years (Hasegawa *et al*. 1979). Dixon (1992) suggests that the southern Beaufort Sea has experienced earthquakes as large as M 6.5. Adams and Atkinson (2003) consider this seismicity potential to be moderate but recent evaluation suggests the potential for large earthquakes (Hyndeman et al. 2005). The Beaufort Sea cluster exhibits normal and strike-slip faulting and extension so not reacting to northerly Yukon block thrust and strike slip motion characterizing the Richardson Mountain

occurrences. The seismicity is thought to be related to crustal tectonic processes and possibly post-glacial isostatic rebound (Dixon, 1992), but Hyndeman et al. (2005) also suggest deeper seated reaction to Mackenzie Delta loading and flexure causing tension. Large-throw normal faulting was recognized on the eastern Beaufort Sea margin on the inner M'Clure Fan (King, 2015), well NE of the seismic cluster. It trends along the shelf-break. The historic record shows sparse seismic events here but they do lie along this faulting trend. The faulting has widespread expression at the seabed and a post-glacial age. Large-scale sediment loading also on the M'Clure Fan is inferred by the topographic build-up into Canada Basin but, to our knowledge, has not been demonstrated with appropriate seismic data. This introduces the possibility that a crustal flexure manifest as extension is active here also. Nevertheless, the mechanism of the offshore events remains unclear.

The concept that synchronous marine sediment failures across a broad area are triggered by earthquakes is demonstrated on the Pacific margin (Adams 1990). This may also apply here. The failures in the KF are spread across a broad area of the Beaufort slope. The general co-location of the broadly distributed failures, the potential for large seismic events (Hyndeman et al. 2005) and the historic 6.4 MN event (Fig. 19) reinforces an inference of triggering by earthquakes. This is compatible with the long history represented by the stacked sequence of MTD's sourced from the Mackenzie Fan and with runout far into Canada Basin (Mosher et al. 2011). The possibility of the failures triggering a tsunami cannot be excluded. Mosher (2009) considered the Ikit failures tsunamigenic potential to be high and our interpretation of the magnitude of initial events is supportive. An initial search for tsunami evidence, including C-14 dating of sand beds in coastal lacustrine deposits bordering the Mackenzie Delta, has been inconclusive (Dallimore, 2015 pers. comm. and internal reporting).

Future Failure

The recurring long-term failure, young age of the most recent MTDs, ubiquity of retrogressive activity, history and clustering of earthquakes and the potential pre-conditioning of remaining unfailed sediment unite to suggest future potential for failure. The unfailed and partially failed sediment on the slope in the KF are most likely to fail in the future. This would depend on the location of the epicentre of any earthquake, the pore pressure conditions in that area, and the sensitivity of silty sediment during cyclic loading. Apparent absence of crown cracks, signaling incipient failure, is curious and perhaps significant. However, micro-faulting above the large headwalls is clear in the CHIRP sub-bottom profiler data collected during AUV surveys (C. Paull, pers. comm.).

STUDY LIMITATIONS, PRESENT AND FUTURE STUDY DIRECTIONS

The absolute age of these upper slope failures and their tsunamigenic potential have not been fully addressed. What are the pre-conditions that make the sediment susceptibility to failure? And a seismic triggering mechanism is speculative and difficult to prove. Until these factors are better known, risk cannot be well assessed.

Focus on the most recent failure ages is currently underway (Cameron et al. 2017). Similarly, a sense of periodicity is being established for the post-glacial record (Riedel, in prep.). Buried failure events are numerous and not necessarily uniformly distributed temporally or spatially. The Riedel study is awaiting completion of a chronological framework tied to seismic horizons for their absolute dating.

The very high resolution AUV imagery shows cross-cutting relationships not discernable with sea-surface-based multibeam systems and demonstrated that they are more complex in their evolution (e.g. Fig 18). Such data coverage in the slide areas is less than 0.5% yet they permit better estimation of the magnitude of the individual events. Clearly, a multi-staged failure introduces more time and diminishes the tsunamigenic potential. Nevertheless, the late-stage events tend to be smaller failures, likely not as tsunamigenic. Repeat surveys have been conducted at two sites and cores collected for dating purposes.

The geographic extent limitations of this study can be addressed with further surveying to deeper water depths; even non-contiguous multibeam coverage would better delineate the size and run-out of failure events. Some of the thick and discrete lensoid mass transport deposits with long run-out distances recognized in the deep water of Canada Basin present a straightforward superposition on sub-bottom profiler data and could be traced back to their slope origins. Further, the margins of such debrites, where they interbed with undisturbed strata, present ideal coring targets, locally buried only a few metres, offering access for much better constrained absolute timing.

The stratigraphic imaging restriction to shallow depths below seabed precludes examination of these deeply cut and filled valleys. This can be addressed through examination of the 3-D seismic data which cover about one half of the area. Inability to recognize the full failure volume may be quite serious with respect to the tsunamigenic potential. Indeed, cursory examination of the 3-D data demonstrates that large and small mass transport is ubiquitous both spatially and though time. These and the mega-failures beyond the immediate study area (Mosher et al. 2011) underscore the need for even the most basic sense of magnitude, density, frequency distribution, source area(s) and, of course, age.

Recognition of possible pre-conditioning of the sediment for failure susceptibility is hampered by the inability to reach appropriate sample depths. Several downslope transects comprising three to four core sites have been analysed from a geotechnical standpoint (MacKillop 2015) but publication awaits a context provided by basic core and shallow seismic and a chronologic framework. The geotechnical information at hand (~65 Atterberg tests) is from the shallow reaches, typically not beyond about 6 m below seabed. These do not particularly distinguish themselves from normal marine and glacimarine muds in a geotechnical sense. They are typically fat clays (CH) with high plasticity, high liquid limit with liquidity indices near unity and consolidations and compressibility reflecting relatively high porosities (Blasco et al. 2011, Table 2.2.2.11 and MacKillop et al. 2015). Yet samples beneath the 10 to 20 m thick, well stratified sediment package are not extant. We suspect the more deeply buried

muds are weaker but this is based on very limited measurement (showing under-consolidation, but in a distant location) and inference from seismic data. The sub-bottom profiler signatures indicate disarticulation and flow of the more deeply buried muds at headwalls while in many cases overlying muds remain intact, “floating” on their substrate until their foundation collapses. The limited geotechnical analyses are being applied to assess a factor of safety (FOS) index towards a risk assessment. Still, the depth and limited distribution of analysis sites may be a further limiting factor. There is some evidence (again, outside the current study scope) for more numerous young failure events on lower, distal slopes compared to higher (shelf edge) slopes, initially contrary to intuition. This suggests a non-uniform sediment susceptibility and complicates extrapolation of a FOS assessment.

A further factor that may be significant is widespread anomalously high negative porewater salinity and sulfate gradients (strong freshing gradients at shallow depth below seabed) and very light $\delta^{18}O$ values measured in slope-situated cores (Gwiazda et al. 2014, Paull et al. 2015a). These indicate a mixing trend between seawater and meteoric waters. The origin of the meteoric signature is a topic of discussion. Fresh porewater is a major factor in failure susceptibility of sediments diagenetically "washed" of originally saline porewater, as are quick clays. Nonetheless, the fresh porewater has to be derived from depth and experiencing upward flux, so the geotechnical character of glacigenic muds buried beyond reach of sampling may induce different stability behavior. Furthermore, initial chronologic investigations matching radiocarbon dated cores and sub-bottom profiler-traced horizons show diminished sedimentation rates in the later deglaciation stages, locally by an order of magnitude. Both the salinity and sedimentation rate factors are probably significant for porewater governing of stability behavior in the more deeply buried muds.

Beaufort Sea margin-wide similarities (and differences) in slope failure size and distribution, as they become better revealed, will provide a context for the slide complexes in this study. Setting differences are already in evidence, for example glaciated trough mouths vs. un-glaciated or short-lived glaciated shelf-break settings. If large slides are widespread across the Beaufort margin, what does this mean with respect to the seismicity cluster? Is it the controlling factor? Have past large seismic events occurred, triggering very widespread failures? Or is the tectonic setting varied across a wider geography and with far less frequent events in some sectors?

SUMMARY AND CONCLUSIONS

This work showcases two large slope-situated mass failures, Ikit and Kugmallit Slide Valley Complexes, each with deeply cut valleys that head at the shelf-break and upper slope. They are considered as individual events but sparse profile data further downslope suggests the may be one broad failure event.

The initial Ikit and Kugmallit Slide Valley Complex events are primarily evacuational in the study area (Fig. 4). These initial events cut the deepest, providing over steepened walls and major

retrogressive failures (Fig. 20). Their downslope mass transport deposits are also recognized, where they are expressed as dominantly elongate bodies.

The slide volumes estimated exceed 50 and 100 km^3 for Ikit and Kugmallit respectively. This pales with respect to older failures in Canada Basin, Mosher et al. (2011), but it does confirm a long and continued episodic failure history. As measured, these are mid-size in accordance with the global assemblage (e.g. Masson et al. 2006, Talling et al. 2014) but if they prove to be contiguous in their deeper (unsurveyed) reaches, they may rank much higher.

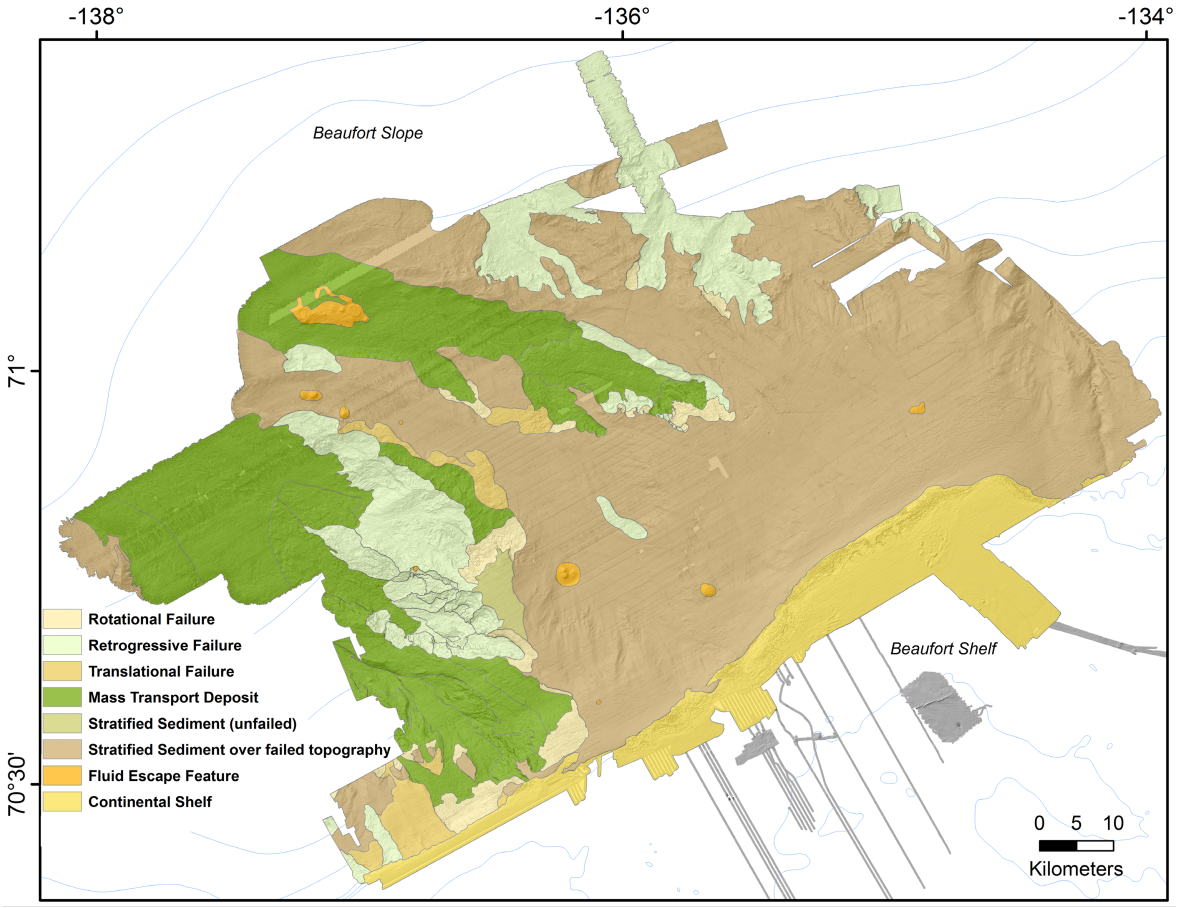

Figure 20 ***Geological process map showing mass transport deposits, types of failures, stratified sediment, continental shelf and fluid escape features. Mass transport deposits are found in all failure areas where sediment evacuation is not complete. Individual failures or deposits are recognized and outlined with gray lines within areas.***

We have recognized retrogressive failure as a typical mechanism to major evacuation, with resulting oversteepening by removal of confining material. At least six successive retrogressive events have been recognized. Translational and rotational failures have been recognized and are found near the top or along the flanks of the slide valleys (Fig 20). If a tsunami was generated, it was during major evacuation events.

We have also recognized several examples of failed flows flanking the slide valley complex that have subsequently failed further, likely through oversteepening by sidewall retrogressive activity. This

means that even sediments that once flowed, reached gravitational equilibrium and came to rest, can still be remobilized.

The slide valley complexes are recent in age, as the lack of a recognizable sediment cover confirms. Headwall cutting of the latest Holocene strata and limited C-14 dating of parent sediments suggest an age less than 1000 yr. Initial Pb and Cs sediment rates (ongoing studies, e.g. Cameron et al. 2017) indicate this could be as recent as several hundred years. Corroborating multiple site reproducibility and further sedimentological investigation to better distinguish unfailed parent block from overlying post-failure sediment is necessary for better substantiation. Failure periodicity is being addressed on the longer term (post-glacial) but results await a chronological framework. The longer history is also expected to contribute to process understanding.

Fluid flux (including gas) to the seabed is manifest in features adjacent and overlapping the SVCs (mud volcanoes, pingos, slide headwalls). Furthermore, a fresher than normal porewater presence in parent sediments even beyond these features. The relative influence from long traveled meteoric, more local but deep permafrost melt, deep hydrate dissociation, local deep formation conduits, and porewater overpressures from rapid sedimentation of fluids is not known. This prevalence of fluid flux makes it likely that one or the combination of these has a pre-conditioning influence on the slope stability.

Nearby and underlying seismicity is the main suspected trigger, given the cluster of historic events in this local, the historical 6.4 M record and the perceived potential for large earthquakes. If a tsunami was generated, it was with the large, initial events. With numerous successive retrogressive events, even if they followed immediately, some time span is inferred. However, no risk analysis is performed.

Failure and tsunami risk analysis will improve when absolute age dating at multiple sites, periodicity and geotechnical properties in boreholes are available, with a better substantiated seismic triggering scenario.

REFERENCES

Adams, J. and G. Atkinson, 2003. Development of seismic hazard maps for the proposed 2005 edition of the National Building Code of Canada. Canadian Journal of Civil Engineering, (30), p. 255-271.

Adams, J., 1990. Paleoseismicity of the Cascadia subduction zone: evidence from turbidites off the Oregon-Washington margin. Tectonics, (9), p. 569–583.

Batchelor, C.L., Dowdeswell, J.A. and Pietras, J.T., 2014. Evidence for multiple Quaternary ice advances and fan development from the Amundsen Gulf cross-shelf trough and slope, Canadian Beaufort Sea margin. Marine and Petroleum Geology, (52), 125-143.

Batchelor, C.L., Dowdeswell, J.A. and Pietras, J.T., 2013. Seismic stratigraphy, sedimentary architecture and palaeo-glaciology of the Mackenzie Trough: evidence for two Quaternary ice advances and limited fan development on the western Canadian Beaufort Sea margin. Quaternary Science Reviews, (65),73-87.

Blasco, S., Woodworth-Lynas, C., Rankin, S., Hawkins, J., Dingler, J., 2012. Outer shelf and upper slope seabed dynamics. Canadian Beaufort Sea based on Geological Data. ArcticNet Annual Science Meeting, December 10–13 (Vancouver, B.C. Program with Abstract

Blasco, S., Bennett, R., Brent, T., Burton, M., Campbell, P., Carr, E., Covill, R., Dallimore, S., Davies, E., Hughes-Clarke, J., Issler, D., MacKillop, K., Mazzotti, S., Patton, E., Shearer, J., White, M., 2011. 2010. State of Knowledge: Beaufort Sea Seabed Geohazards Associated with Offshore Hydrocarbon Development; Geological Survey of Canada, Open File 6989, 335 p. https://doi.org/10.4095/292616

Blasco, K.A., Blasco, S.M., Bennett, R., MacLean, B., Rainey, W.A. and Davies, E.H., 2010. Seabed geologic features and processes and their relationship with fluid seeps and the benthic environment in the Northwest Passage. Geological Survey of Canada, Open File 6438, 2010, 58 p., https://doi.org/10.4095/287316

Bringué, M. and Rochon, A., 2012. Late Holocene paleoceanography and climate variability over the Mackenzie slope (Beaufort sea, Canadian Arctic). Marine Geology, (29), 83-96.

Cameron, G.D.M., King, E.L.,Murray, D., Kuzyk, Z.A., and Blasco, S. 2017. Relative timing of sediment failures within slide-valley complexes in the Kugmallit Fan area of the central Beaufort Slope, offshore Northwest Territories. Geological Survey of Canada, Scientific Presentation 74, 1 sheet, https://doi.org/10.4095/306013

Dallimore, S.R. Paull, C.K., Taylor, A.E., Riedel, M., Jin, J.K. and Côté, M.M. 2015. Geohazard investigations of permafrost and gas hydrates in the outer shelf and upper slope of the Canadian Beaufort Sea. GeoQuebec 2015. Extended abstract. Sept. 20-23, Quebec City.

Dallimore, S.R., Paull, C.K., Caress, D.W, Gwiazda, R., Jin, Y.K., Riedel, M., Taylor, A., Lundsten, E. Anderson, K and Melling, H. (in prep.) Submarine Permafrost Processes Along the Western Canadian Arctic Shelf Edge. Geophysical Research Letters.

Paull, C., Dallimore S.R., Caress, D.W, Gwiazda, R., Lundsten, E.M., Anderson, K., Riedel, M., and Melling, H. 2015. Slope Edge Deformation and Permafrost Dynamics Along the Arctic Shelf Edge, Beaufort Sea, Canada. Abstract OS22B-07 presented at 2015 Fall Meeting, AGU, San Francisco, Calif., 14-18 Dec.

Dixon, J., Dietrich, J. R. and. McNeil, D. H., 1992. Upper Cretaceous to Pleistocene Sequence Stratigraphy of the Beaufort-Mackenzie and Banks Island areas, northwest Canada: Geological Survey of Canada Bulletin, (407), p. 90.

DongHun, L., YoungKeun, J., JungHyun, K., Heldge, N., JongKu, G. and BoHyung, C., 2016, Organic geochemical signatures controlling methane outgassing at active mud volcanoes in the Canadian Beaufort Sea. *In*: EGU General Assembly Conference Abstracts, (18), p. 1159, April, 2016.

Duk-Rodkin, A. and Hughes, O.L. 1994. Tertiary-Quaternary drainage of the pre glacial Mackenzie Basin. Quaternary International, 22/23, 221-241.

Dyke, A.S., Moore, A. & Robertson, L., 2003. Deglaciation of North America. Geological Survey of Canada Open File, 1574. Thirty-two digital maps at 1:7,000,000 scale with accompanying digital chronological database and one poster (two sheets) with full map series.

Frederick, J.M. 2015. Effects of submarine groundwater discharge on the present‐day extent of relict submarine permafrost and gas hydrate stability on the Beaufort Sea continental shelf, Journal of geophysical research. (120), 3, p. 417. DOI: 10.1002/2014JF003349

Geissler, W.H., Gebhardt, A.C., Gross, F., Wollenburg, J., Jensen, L., Schmidt-Aursch, M.-C., Krastel, S., Elger, J.,and Osti, G. 2016. Arctic megaslide at presumed rest. Sci. Rep. 6, 38529; doi: 10.1038/srep38529

Grantz, A., Hart, P.E., and Childers, V.A.. 2011. Geology and tectonic development of the Amerasia and Canada Basins, Arctic Ocean: *In:* Spencer A.M., Gautier D., Stoupakova A., Embry A., Sorensen K. (eds) Arctic Petroleum Geology Geological Society of London Memoirs, (35), 771-799.

Gwiazda, R., C. K. Paull, Dallimore, S., Melling, H., and Jin, Y. K. 2014. Distinctive sources of fluids in different environments of the Beaufort Sea seafloor, Abstract OS12A-06 presented at 2014 Fall Meeting, AGU, San Francisco, California., 15–19 Dec.

Halchuk, S., Allen, T. I., Rogers, G.C. and Adams, J. 2015. Seismic Hazard Earthquake Epicentre File (SHEEF2010) used in the fifth generation seismic hazard maps of Canada. Geological Survey of Canada, Open File 7724.

Hill, P.R., Mudie, J.P., Moran, K., Blasco, S.M., 1985. A sea-level curve for the Canadian Beaufort Shelf. Canadian Journal of Earth Sciences, (22), p. 1383 – 1393.

Harris, P.T., MacMillan-Lawler, M., Rupp, J., Baker, E.K., 2014. Geomorphology of the oceans. Marine Geology, (352), p. 4-24.

Hart, P.E., Pohlman J.W., Lorenson T.D., and Edwards B.D. 2011. Beaufort sea deep-water gas hydrate recovery from a seafloor mound in a region of widespread BSR occurrence. *In*: Proceedings of the 7th International Conference on Gas Hydrates (ICGH 2011), Edinburgh, Scotland, 2011.

Hyndman, R.D., Cassidy, J.F. , Adams, J., Rogers, G.C., and Mazzotti, S. 2005. Earthquakes and Seismic Hazard in the Yukon-Beaufort-Mackenzie. Recorder, Canadian Society of Exploration Geophysicists, (30), 5.

Jin, Y.K., Riedel, M., Hong, J.K., Nam, S.I., Jung, J.Y., Ha, S.Y., Lee, J.Y., Kim, G.Y., Yoo, J., Kim, H.S. and Kim, G., 2015. Overview of field operations during a 2013 research expedition to the southern Beaufort Sea on the RV Araon.

Jin, Y.K., Côté, M.M., Paull, C.K., and King, E.L. (ed.), 2018. 2017 Korea-Canada-U.S.A. Beaufort Sea (offshore Yukon and Northwest Territories) research program: 2017 Araon expedition (ARA08C) cruise report; Geological Survey of Canada, Open File 8406, 206 p. https://doi.org/10.4095/308396

King, E.L.2015. Late glaciation in the eastern Beaufort Sea: contrasts in shallow depositional styles from Amundsen Gulf, Banks Island Shelf and M'Clure Strait. Abstract in, ArcticNet Annual Scientific Meeting, p. 63, , Dec. 2015, Vancouver. (ESS Cont.# 20150335) http://www.arcticnetmeetings.ca/asm2015/docs/topical-abstracts.pdf

King, E.L., Li, M., Wu, Y., Forest, A., Blasco, S., Harrison, P., Robertson, A, Melling, H., Dallimore, S.R., Paull, C.K. and Cameron, G.D.M. 2017. A belt of seabed erosion along the Beaufort Sea margin, offshore Northwest Territories, governed by Holocene evolution of the Beaufort Shelf-Break Jet; geological evidence, current measurements, and initial oceanographic modelling. Geological Survey of Canada, Open File 8198, 2017, 1 sheet, https://doi.org/10.4095/299691

Lafuerza, S., Sultan, N., Canals, M., Lastras, G., Cattaneo, A, Frigola, J., Costa, S., and Berndt, C., 2012. Failure mechanisms of Ana Slide from geotechnical evidence, Eivissa Channel, Western Mediterranean Sea. Marine Geology, (307), p. 1–21.

Lamontagne, M., Halchuk, S., Cassidy, J.F., and Rogers, G.C., 2008. Significant Canadian earthquakes of the period 1600–2006: Seismological Research Letters, (79), p. 211-223.

Melling, H. and cruise participants. 2013. Beaufort Marine Hazards: 2013 Field Expedition Report. September 25 – October 16, 2013. Institute of Ocean Sciences Cruise 2013-22 Pacific Geoscience Centre Cruise 2013-005. Joint Report by Fisheries and Oceans Canada, Geological Survey of Canada and Monterey Bay Aquarium Research Institute. https://www.google.ca/search?q=Beaufort+Marine+Hazards&rlz=1C1GCEA_enCA751CA751&oq=Beaufort+Marine+Hazards&aqs=chrome..69i57.1534j0j8&sourceid=chrome&ie=UTF-8

MacKillop, K., King, E.L., Cameron, G.D.M. and Blasco, S. 2015. Seabed stability on the Beaufort Slope: Sediment geotechnical characterization and geologic context. Abstract. Annual Arcticnet Science Meeting, Dec. 2015, Vancouver. http://www.arcticnetmeetings.ca/asm2015/docs/posters-abstracts.pdf

Masson, D.G., Harbitz, C.B., Wynn, R.B., Pedersen, G. and Løvholt, F., 2006. Submarine landslides: processes, triggers and hazard prediction. Philosophical Transactions of the Royal Society of London A: Mathematical, Physical and Engineering Sciences, (364), 1845, 2009-2039.

Melling, H. and field participants. 2013. Beaufort Marine Hazards, CCGS Sir Wilfrid Laurier, September 25 – October 16, 2013. Fisheries and Oceans Canada, Natural Resources Canada and Monterey Bay Research Aquarium Technical Report. IOS Expedition number 2013-22, 36p.

Mosher, D.C., 2009. Submarine landslides and consequent tsunamis in Canada, Geoscience Canada, (36), 4, p. 179-190.

Mosher, D.C., Shimeld, J.W., Hutchinson, D., Lebedeva-Ivanova, N, and Chapman, C.B., 2011. Submarine Landslides in Arctic Sedimentation: Canada Basin. *In:* Yamada, Y., Kawamura, K., Ikehara, K., Ogawa, Y., Urgeles, R., Mosher, D., Chaytor, J. and Strasser, M. (eds). Submarine Mass Movements and Their Consequences V, Advances in Natural and Technological Hazards Research, (29), 9 p.

Murton, J.B., Bateman, M.D., Waller, R.I. 2015. Late Wisconsin glaciation of Hadwen and Summer islands, Tuktoyaktuk Coastlands, NWT, Canada. GeoQuebec In: C.R.Burn, editor, Proceedings of a Symposium to Commemorate the Contributions of Professor J. Ross Mackay (1915-2014) to Permafrost Science in Canada. 20-23 September 2015, Quebec City.

Paull, C.K., Caress, D.W., Thomas, H., Lundsten, E., Anderson, K., Gwiazda, R., Riedel, M., McGann, M., and Herguera, J.C. 2015b. Seafloor geomorphic manifestations of gas venting and shallow subbottom gas hydrate occurrences. Geosphere, (11), 2, p. 491–513. doi: https://doi.org/10.1130/GES01012.1

Paull, C.K., Dallimore, S. R., Caress, D.W., Gwiazda, R., Melling, H., Riedel, M., Jin, Y. K., Hong, J. K., Kim, Y.-G., Graves, D., Sherman, A., Lundsten, E., Anderson, K., Lundsten, L., Villinger, H, Kopf, A., Johnson, S. B., Hughes Clarke, J., Blasco, S., Conway, K., Neelands, P., Thomas, H., and Côté, M. 2015a. Active mud volcanoes on the continental slope of the Canadian Beaufort Sea, Geochemistry, Geophysics, Geosystems, (16), 9, p. 3160–3181. doi:10.1002/2015GC005928.

Paull, C., Dallimore, S., Hughes-Clarke,J., Blasco, S., Lundsten, E., Ussler III, W., Graves, D., Sherman, A., Conway, K., Melling, H., Vagle, S., and Collett. T. 2011. Tracking the decomposition of submarine permafrost and gas hydrate under the shelf and slope of the Beaufort Sea. Paper 328 in the Special Session - Gas Hydrates & Global Climate Change, 17-21 July 2011, Edinburgh, Scotland.

Paull, C.K, Ussler, W., Dallimore, S.D., Blasco, S.M., Lorenson, T.D., Melling, H., Medioli, B.E., Nixon F.M. and McLaughlin, F.A. 2007. Origin of pingo-like features on the Beaufort Sea Shelf and their possible relationship to decomposing methane gas hydrates. Geophysical Research Letters, (34), p. 1-5.

Piper, D.J.W., Cochonat, P. and Morrison, M.L. 1999. Sidescan sonar evidence for progressive evolution of submarine failure into a turbidity current: the 1929 Grand Banks event. Sedimentology, (46), 79-97.

Rampton V.N. 1982. Quaternary Geology of the Yukon Coastal Plain. Geological Survey of Canada, Bulletin (317), 49 p (4 sheets), https://doi.org/10.4095/111347

Rampton, V. N. 1988. Quaternary Geology of the Tuktoyaktuk Coastlands, Northwest Territories; Geological Survey of Canada, Memoir (423), 1988, 98 p.

Riedel M., Conway, K.W., King, E.L. Cameron, G.D.M. Blasco, S., Jin, Y.K., Hong J.K., Dallimore, S.R. (in prep.) A chronology of mass-transport deposits along the Canadian Beaufort Sea margin – implications for geohazards.

Riedel, M., Brent, T.A., Taylor, G., Taylor, A.E., Hong, J.-K., Jin, Y.-K., and Dallimore, S.R. 2017. Evidence for gas hydrate occurrences in the Canadian Arctic Beaufort Sea within permafrost-associated shelf and deep-water marine environments, Marine and Petroleum Geology, 81, 66-78 doi.org/10.1016/j.marpetgeo.2016.12.027

Riedel M., Taylor G., Taylor A.E. and Dallimore S.R. 2015. Evidence for a deep gas hydrate stability zone associated with submerged permafrost on the Canadian Arctic Beaufort Shelf, Northwest Territories. Geological Survey of Canada Current Research.

Rohr, K.M.M., Riedel, M. and Dallimore, S.R., (in prep). Slope fan and glacial sedimentation on the central Beaufort continental slope, Arctic Canada.

Saint-Ange, F., Kuss, P., Blasco, S., Piper, D.J.W., Clarke, J.H., Mackillop, K., 2014. Multiple failure styles related to shallow gas and fluid venting, upper slope Canadian Beaufort Sea, northern Canada. Marine Geology, (355), 136-149 p.

Talling, P.J., M. Clare, M. Urlaub, E. Pope, J.E. Hunt, and S.F.L. Watt. 2014. Large submarine landslides on continental slopes: Geohazards, methane release, and climate change. Oceanography 27(2):32–45, http://dx.doi.org/10.5670/oceanog.2014.38.

Winkelmann, D. & Stein, R. 2007. Triggering of the Hinlopen/Yermak Megaslide in relation to paleoceanography and climate history of the continental margin north of Spitsbergen. Geochemistry, Geophysics, Geosystems (8), 6, Q06018.

Woodworth-Lynas, C., Blasco, S, Duff, D., Fowler, J., Isler, E.B., Landva, J., Cumming, E., Caines, A, and Smith, C. 2016. Regional assessment of seabed geohazard conditions Canadian Beaufort outer shelf and upper slope: legacy data synthesis: section 2, geophysical and geological data compilation, outer shelf and upper slope southern Beaufort Sea: a handbook of geohazard conditions. Environmental Studies Research Fund Report 208-2 https://www.esrfunds.org/sites/www.esrfunds.org/files/publications/ESRF208-2-Woodworth-Lynas-Blasco.pdf